Supplementary Information for

# Isomerism of the Rhombic Fe$_4$ core in the Zintl Clusters [Fe$_4$E$_{18}$]$^{4-}$ (E = Sn and Pb)

## Table of Contents

## 1. Experimental Procedures

Synthesis of **[K(2,2,2-crypt)]$_4$[Fe$_4$Sn$_{18}$]·4DMF (1-DMF)**

In a 10 mL vial, K$_4$Sn$_9$ (122 mg, 0.1 mmol) and 2.2.2-crypt (115mg, 0.3 mmol) were dissolved in en (ca. 3 mL) and stirred for 30 min, resulting a dark brown solution. Then FeCp$_2$ (30 mg, 0.160 mmol) was dispersed in toluene (0.5 mL), producing a light pink suspension, and then added dropwise to the above mixture. The mixture was stirred for 3 h at room temperature yielding a brown solution. All volatiles were removed at 60°C under vacuum to obtain black solid which was dissolved in 3mL DMF. The resulting green-black solution was stirred for 1 h at room temperature and filtered with glass wool. The filtrate was layered with 3 mL toluene. A large number of brown plate-like crystals of **1-DMF** were obtained (17% yield based on the used precursor K$_4$Sn$_9$) after one week.

## 2. Crystallographic details

The structure of crystals **1**, **1-DMF** and **2** were solved using direct methods and then refined using SHELXL-2014 and Olex2[1-3] to convergence, in which all the non-hydrogen atoms were refined anisotropically during the final cycles. All hydrogen atoms of the organic molecule were placed by geometrical considerations and were added to the structure factor calculation. We used the PLATON SQUEEZE procedure[4] to remove the solvent molecules which could not be modeled properly. A summary of the crystallographic data for the title compounds was listed in table S1. CCDC entries 2206397 (**1**), 2170117 (**1-DMF**), and 2101583 (**2**) are included in the supplementary crystallographic data for this paper. These data can be obtained free of charge from The Cambridge Crystallographic Data Centre (www.ccdc.cam.ac.uk/data_request/cif).

**Table S1.** X-ray measurements and structure solutions of **1**, **1-DMF**, and **2**.

| Compound | **1** | **1-DMF** | **2** |
|---|---|---|---|
| CCDC number | 2206397 | 2170117 | 2101583 |
| Empirical formula | $C_{92}H_{164}Fe_4K_4N_{12}O_{24}Sn_{18}$ | $C_{42}H_{86}Fe_2K_2N_6O_{14}Sn_9$ | $C_{46}H_{82}N_6O_{12}K_2Fe_2Pb_9$ |
| Formula weight | 4338.56 | 2157.27 | 2965.78 |
| Temperature/K | 100.01(11) | 129.99(10) | 100.00(10) |
| Crystal system | monoclinic | triclinic | monoclinic |
| Space group | $P2_1/n$ | $P$-1 | $P2_1/n$ |
| $a$ /Å | 14.30740(10) | 15.7369(2) | 14.3298(1) |
| $b$ /Å | 27.4645(2) | 15.9735(3) | 27.6726(2) |
| $c$ /Å | 18.80560(10) | 16.6129(2) | 18.9178(2) |
| $\alpha$/° | 90 | 107.7610(14) | 90 |
| $\beta$/° | 110.6780(10) | 97.0389(12) | 110.718(1) |
| $\gamma$/° | 90 | 112.8799(15) | 90 |
| V /Å$^3$ | 6913.54(9) | 3522.99(10) | 7016.60(11) |
| Z | 2 | 2 | 4 |
| $\rho_{calc}$ /g·cm$^{-3}$ | 2.084 | 2.034 | 2.808 |
| $\mu(Cu_{K\alpha})$ /mm$^{-1}$ | 30.148 | 29.596 | 45.713 |
| $F(000)$ | 4144.0 | 2064.0 | 5296.0 |
| $2\Theta$ range /° | 7.346 to 133.998 | 8.38 to 133.998 | 7.328 to 133.996 |
| Reflections collected / unique | 34230 / 12283 | 34014 | 35931 |
| Data / restraints / parameters | 12283 / 2094 / 749 | 12507 / 25 / 680 | 12483 / 0 / 694 |
| $R_1$/$wR_2$ ($I$>2σ($I$))[a] | $R_1$ = 0.0368, $wR_2$ = 0.0886 | $R_1$ = 0.0518, $wR_2$ = 0.1385 | $R_1$ = 0.0597, $wR_2$ = 0.1603 |
| $R_1$/$wR_2$ (all data) | $R_1$ = 0.0472, $wR_2$ = 0.0921 | $R_1$ = 0.0568, $wR_2$ = 0.1423 | $R_1$ = 0.0665, $wR_2$ = 0.1658 |
| $GooF$ (all data)[b] | 1.016 | 1.034 | 1.017 |
| Max. peak/hole /e$^-$·Å$^{-3}$ | 1.95 / -1.29 | 3.49 / -1.57 | 4.43 / -2.77 |
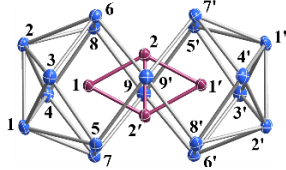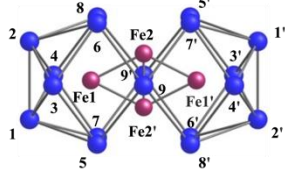
[a] $R_1 = \sum||F_o|-|F_c||/\sum|F_o|$; $wR_2 = \{\sum w[(F_o)^2-(F_c)^2]^2/\sum w[(F_o)^2]^2\}^{1/2}$

[b] $GooF = \{\sum w[(F_o)^2-(F_c)^2]^2/(n-p)\}^{1/2}$

**Table S2.** Selected bond lengths (in Å) of the experiment (in **1-DMF**) and optimized geometries of $^{11}B_{3g}$-[Fe$_4$@Sn$_{18}$]$^{4-}$ at the M06-L/TZ2P level of theory.

| | Experimental | $^{11}B_{3g}$-[Fe$_4$@Sn$_{18}$]$^{4-}$ |
|---|---|---|
| |  |  |
| Sn1–Sn2 | 3.0436(7) | 3.09 |
| Sn1–Sn3 | 3.0544(7) | 3.08 |
| Sn1–Sn4 | 3.0355(7) | |
| Sn2–Sn3 | 3.0411(7) | |
| Sn2–Sn4 | 3.0562(7) | |
| Sn1–Sn5 | 3.1176(7) | 3.17 |
| Sn1–Sn7 | 3.1420(7) | |
| Sn2–Sn6 | 3.1361(7) | |
| Sn2–Sn8 | 3.1207(7) | |
| Sn3–Sn5 | 3.0441(7) | 3.12 |
| Sn3–Sn6 | 3.0487(7) | |
| Sn4–Sn7 | 3.0460(7) | |
| Sn4–Sn8 | 3.0722(7) | |
| Sn5–Sn7 | 3.0184(7) | 3.09 |
| Sn6–Sn8 | 3.0245(7) | |
| Sn5–Sn9' | 3.2511(7) | 3.24 |
| Sn6–Sn9' | 3.2157(7) | |
| Sn7–Sn9 | 3.2179(7) | |
| Sn8–Sn9 | 3.2291(7) | |
| Fe1–Fe2 | 2.4315(14) | 2.41 |
| Fe1–Fe2' | 2.4309(14) | |
| Fe2–Fe2' | 2.500(2) | 2.52 |
| Fe1–Sn1 | 2.8637(11) | 2.87 |
| Fe1–Sn2 | 2.8535(11) | |
| Fe1–Sn3 | 2.8345(11) | 2.88 |
| Fe1–Sn4 | 2.8349(11) | |
| Fe1–Sn5 | 2.8612(11) | 2.93 |
| Fe1–Sn6 | 2.8618(11) | |
| Fe1–Sn7 | 2.8644(11) | |
| Fe1–Sn8 | 2.8674(11) | |
| Fe2'–Sn5 | 2.7182(11) | 2.72 |
| Fe2'–Sn7 | 2.7150(11) | |
| Fe2–Sn8 | 2.7017(12) | |
| Fe2–Sn9 | 2.7176(12) | 2.75 |
| Fe2'–Sn9 | 2.7522(12) | |

**Table S3.** Selected bond lengths (in Å) of the experiment and optimized geometries of $^{11}B_{1g}$-[Fe$_4$@Pb$_{18}$]$^{4-}$ at the M06-L/TZ2P level of theory.

| | Experimental | $^{11}B_{1g}$-[Fe$_4$@Pb$_{18}$]$^{4-}$ |
|---|---|---|
| |  |  |
| Pb1–Pb2 | 3.1784(7) | 3.22 |
| Pb1–Pb3 | 3.1394(7) | 3.24 |
| Pb1–Pb4 | 3.1653(7) | |
| Pb2–Pb3 | 3.1418(6) | |
| Pb2–Pb4 | 3.1527(7) | |
| Pb1–Pb5 | 3.2322(6) | 3.35 |
| Pb1–Pb7 | 3.2706(7) | |
| Pb2–Pb6 | 3.2848(6) | |
| Pb2–Pb8 | 3.2472(7) | |
| Pb3–Pb5 | 3.1892(7) | 3.24 |
| Pb3–Pb6 | 3.1551(7) | |
| Pb4–Pb7 | 3.1669(7) | |
| Pb4–Pb8 | 3.1771(7) | |
| Pb5–Pb7 | 3.2091(7) | 3.28 |
| Pb6–Pb8 | 3.2232(7) | |
| Pb5–Pb9' | 3.2866(7) | 3.32 |
| Pb6–Pb9' | 3.2747(7) | |
| Pb7–Pb9 | 3.2864(7) | |
| Pb8–Pb9 | 3.2580(7) | |
| Fe1–Fe2 | 2.431(2) | 2.44 |
| Fe1–Fe2' | 2.437(2) | |
| Fe2–Fe2' | 2.328(4) | 2.29 |
| Fe1–Pb1 | 2.9241(18) | 2.97 |
| Fe1–Pb2 | 2.9311(17) | |
| Fe1–Pb3 | 2.9734(19) | 3.03 |
| Fe1–Pb4 | 2.9742(18) | |
| Fe1–Pb5 | 2.9413(17) | 3.02 |
| Fe1–Pb6 | 2.9736(19) | |
| Fe1–Pb7 | 2.9578(19) | |
| Fe1–Pb8 | 2.9308(17) | |
| Fe2–Pb5 | 2.7944(19) | 2.85 |
| Fe2–Pb6 | 2.7906(19) | |
| Fe2–Pb7 | 2.8313(19) | |
| Fe2'–Pb8 | 2.8147(18) | |
| Fe2–Pb9 | 2.8729(19) | 2.90 |
| Fe2'–Pb9 | 2.8922(19) | |

**Figure S1.** Crystal image of compounds **1** (left), **1-DMF** (middle) and **2** (right).



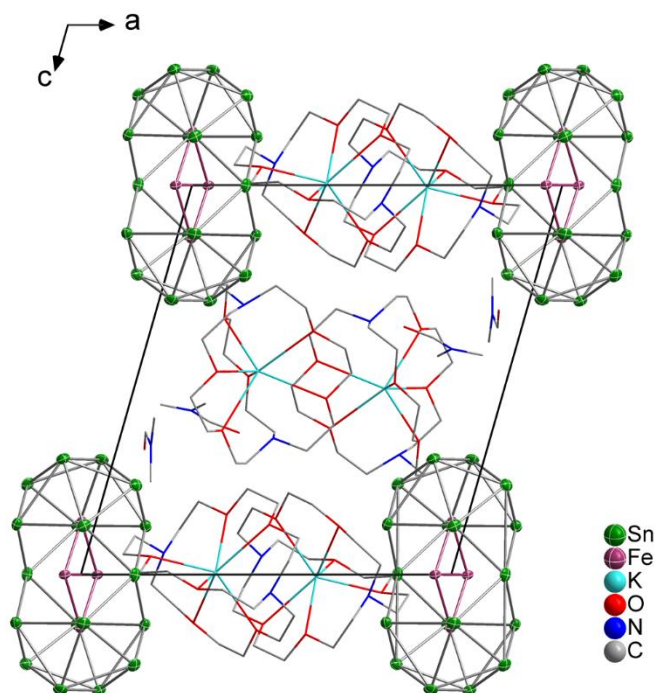| | Sn |
|---|---|
| | Fe |
| | K |
| | O |
| | N |
| | C |
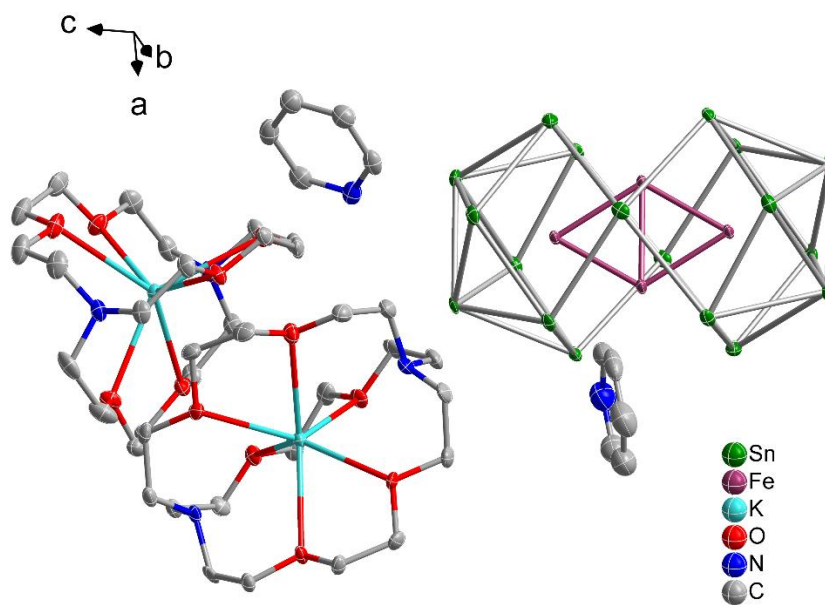
**Figure S2.** Asymmetric unit of **1**. The disorder positions (atoms and bonds) given in semi-transparent mode (60%).
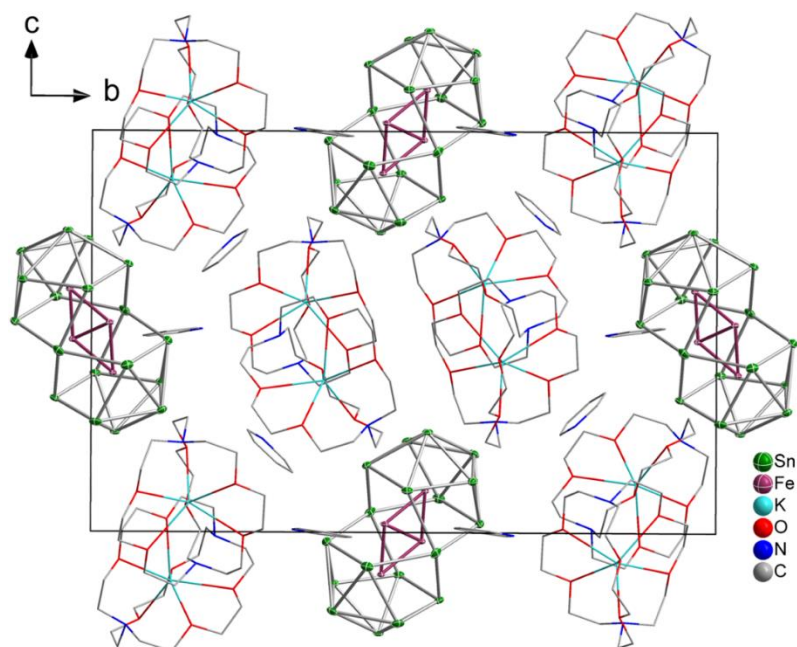
**Figure S3.** View of the unit cell of **1**. The disorder of Sn atoms is omitted here for clarity.
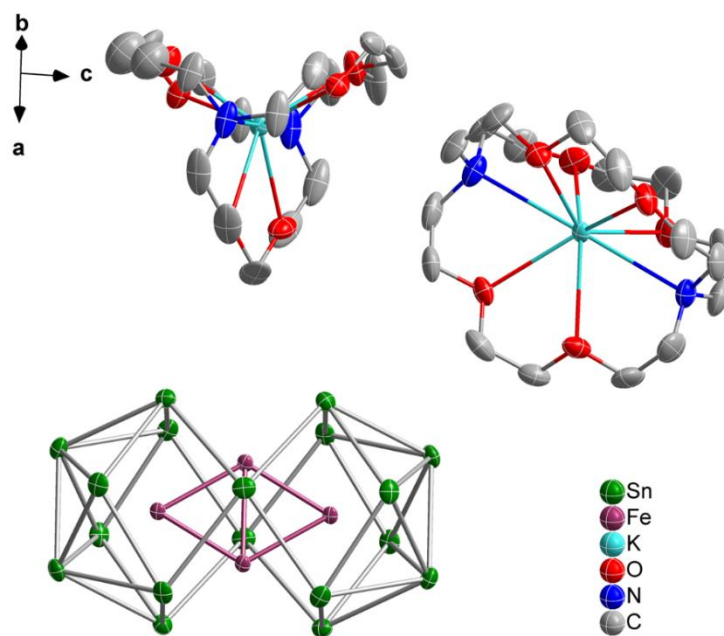


**Figure S4.** Asymmetric unit of **1-DMF**. The minor components (H atoms) in the cluster site are omitted for clarity.

**Figure S5.** View of the unit cell of **1-DMF**. Minor components (H atoms) in the cluster site are omitted for clarity.
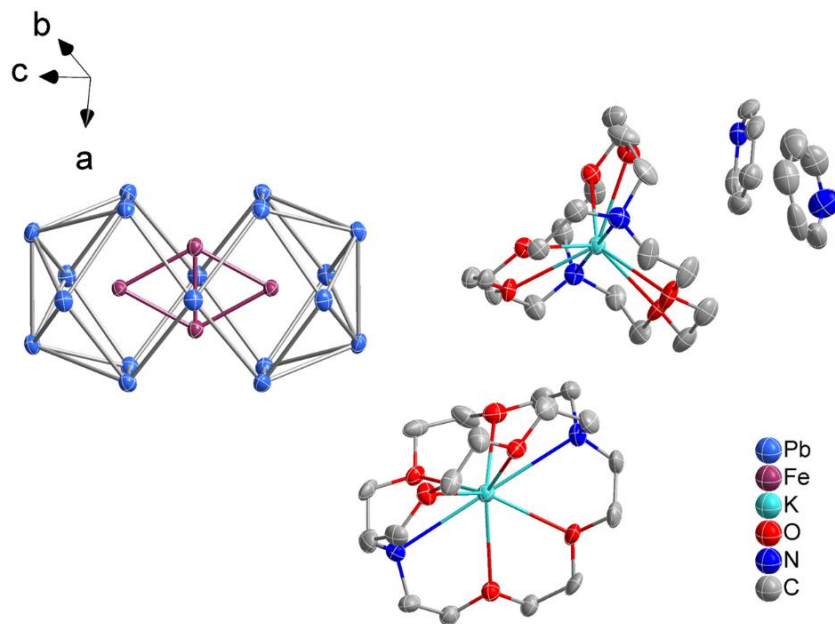


**Figure S6.** Asymmetric unit of **2** with the cluster fragment. Thermal ellipsoids are drawn at 50% probability. The minor components are omitted for clarity.
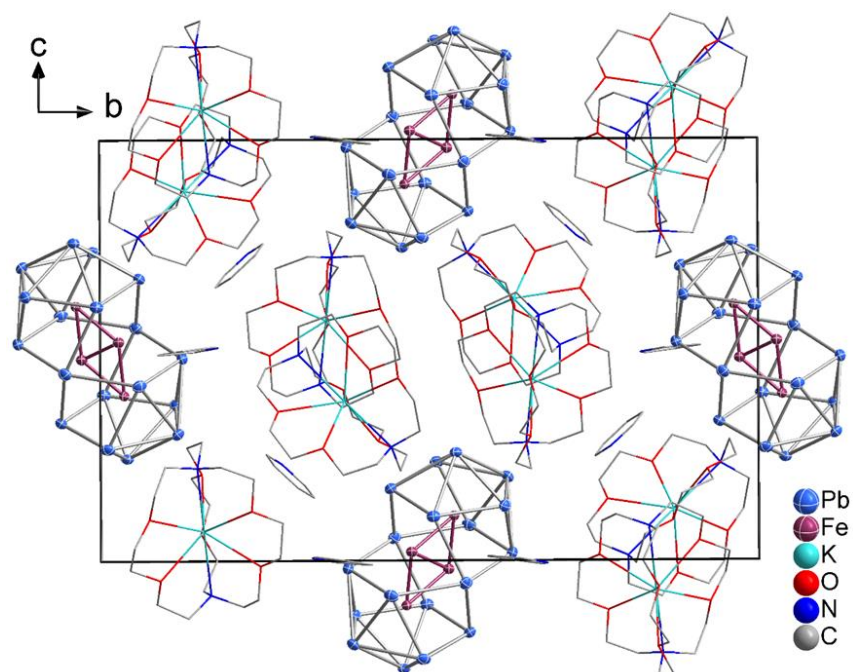
**Figure S7.** View of the unit cell of **2**. Minor components (H atoms) in the cluster site are omitted for clarity.
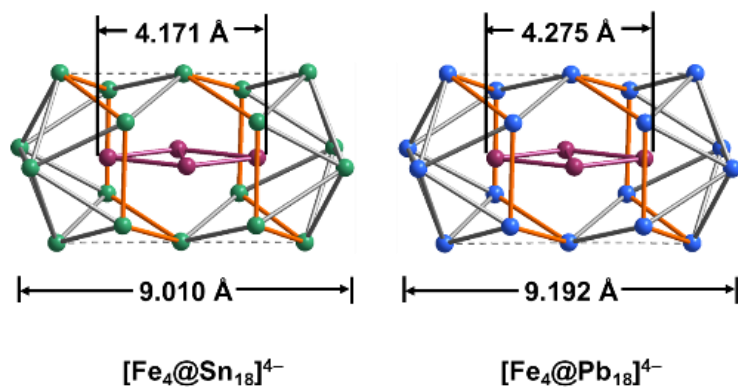


$[Fe_4@Sn_{18}]^{4-}$            $[Fe_4@Pb_{18}]^{4-}$

**Figure S8.** Axial distances of Fe motifs in compounds **1**-**2**, and the dimensions of anions $[Fe_4@Sn_{18}]^{4-}$, and $[Fe_4@Pb_{18}]^{4-}$.

## 3. ESI-MS Studies

The ESI-MS of the DMF solution of the crystals of **1** (Figure S9) and **2** (Figure S13) were performed under the condition of rapid injection in an inert atmosphere, indicating that $[Fe_4@Sn_{18}]^{2-}$ (m/z = 1179.9856), $[Fe_4@Sn_{18}]^{-}$ (m/z = 2359.9674), $[K(2.2.2\text{-crtpt})Fe_4@Sn_{18}]^{-}$ (m/z = 2775.1872), $[Fe_4@Pb_{18}]^{2-}$ (m/z = 1976.6402) and $[Fe@Pb_{12}]^{-}$ (m/z = 2542.6259) are stable in solution. Measured and simulated isotope distributions for all two species are shown in the Figures S10-12, S14, and S15.
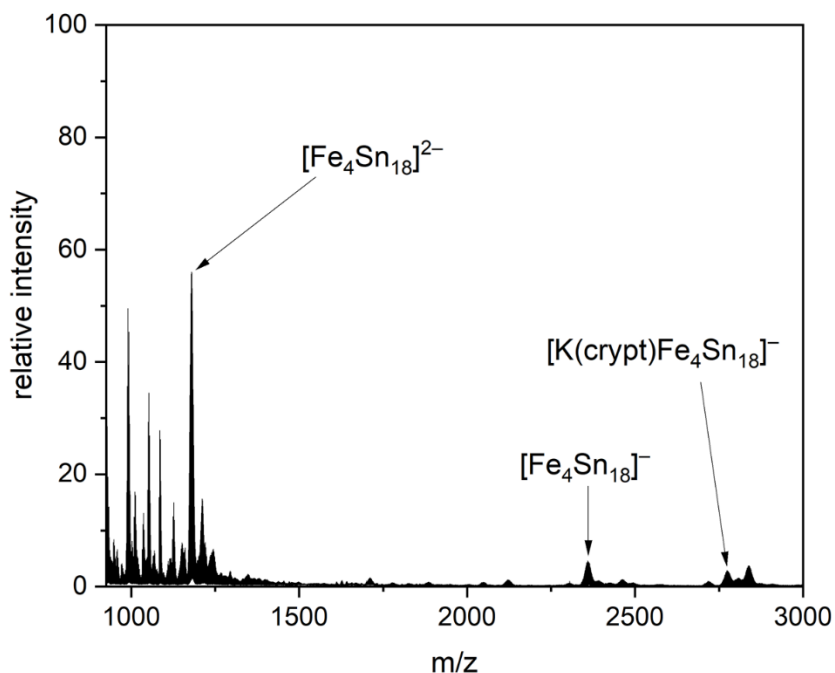


**Figure S9.** Overview ESI mass spectrum in negative ion mode recorded immediately upon injection of a fresh DMF solution of **1**.
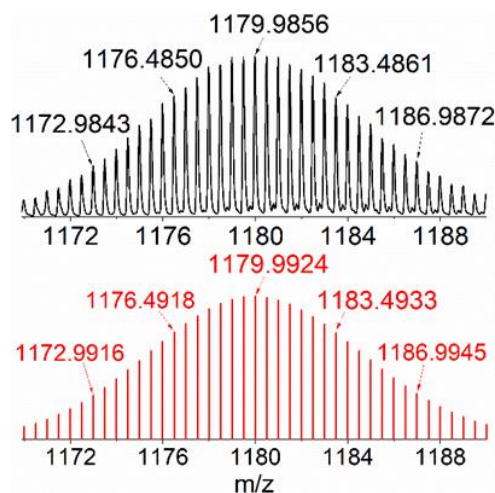


**Figure S10.** Measured (top) and simulated (bottom) spectrum of the fragment $[Fe_4Sn_{18}]^{2-}$.
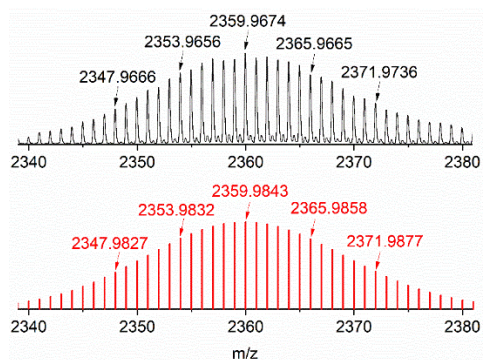
**Figure S11.** Measured (top) and simulated (bottom) spectrum of the fragment $[Fe_4Sn_{18}]^-$.
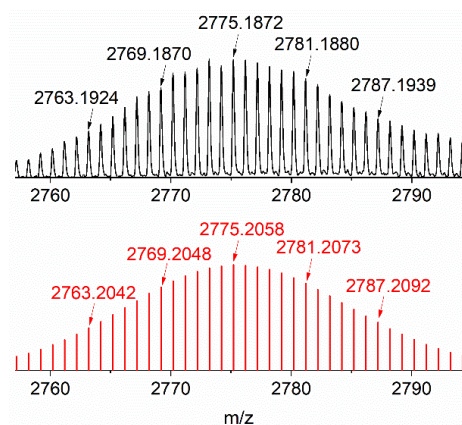


**Figure S12.** Measured (top) and simulated (bottom) spectrum of the fragment $[K(2.2.2\text{-}crtpt)Fe_4Sn_{18}]^-$.
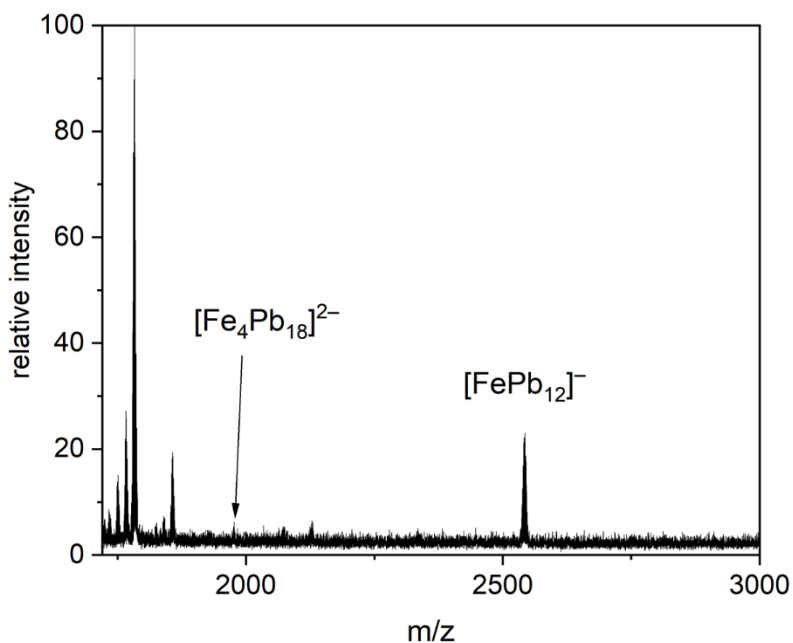


**Figure S13.** Overview ESI mass spectrum in negative ion mode recorded immediately upon injection of a fresh DMF solution of **2**.
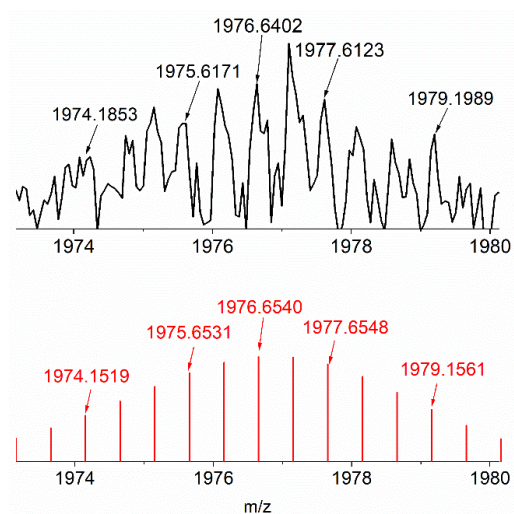
**Figure S14.** Measured (top) and simulated (bottom) spectrum of the fragment $[Fe_4Pb_{18}]^{2-}$.
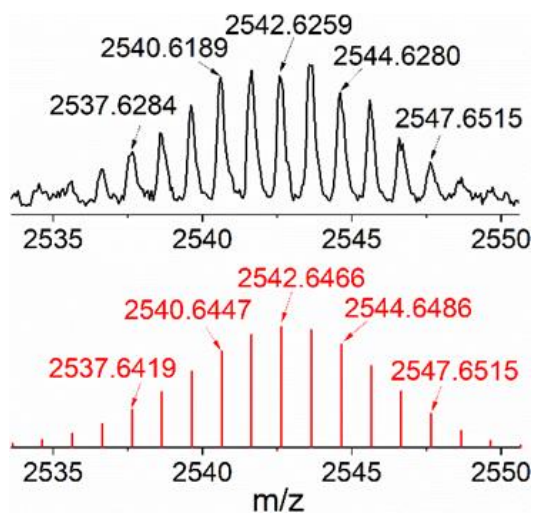


**Figure S15.** Measured (top) and simulated (bottom) spectrum of the fragment $[FePb_{12}]^-$.

## 4. Energy Dispersive X-ray (EDX) Spectroscopic Analysis

EDX analysis on **1** and **2** (Figure S16-S18) was performed by a scanning electron microscope (FE-SEM, JEOL JSM-7800F, Japan). Data acquisition was performed with an acceleration voltage of 15 kV and an accumulation time of 60 s. For **1-DMF** and **2**, a deviation in quantity K was observed in the EDX representation, which may be due to the irregular surface of a crystals after exposure to air.
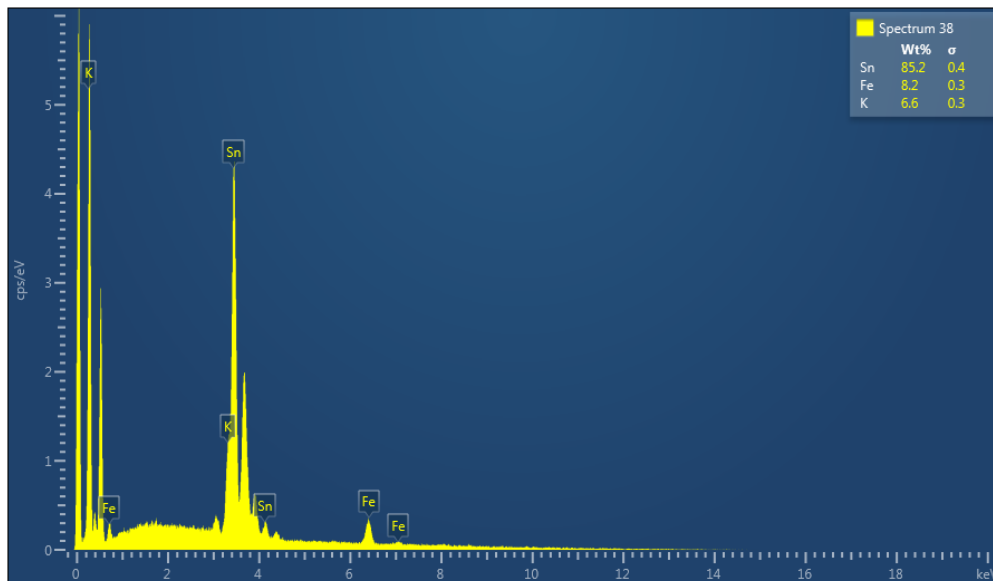


**Figure S16.** EDX analysis of **1**.

| Element | wt% | σ | Observed / Calculated Element Ratio |
|---------|------|-----|------------------------------------|
| K | 6.6 | 0.3 | 4.3/4.0 |
| Fe | 8.2 | 0.3 | 3.7/4.0 |
| Sn | 85.2 | 0.4 | 18.3/18.0 |

13
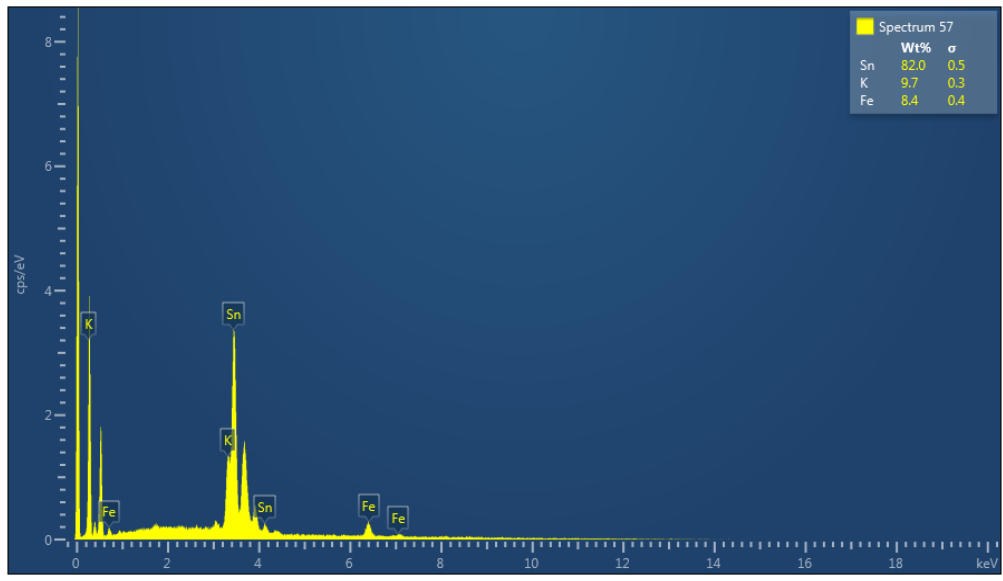
**Figure S17.** EDX analysis of **1-DMF**.

| Element | wt% | σ | Observed / Calculated Element Ratio |
|---------|------|-----|-------------------------------------|
| K | 9.7 | 0.3 | 6.5/4.0 |
| Fe | 8.4 | 0.4 | 3.9/4.0 |
| Sn | 82.0 | 0.5 | 18.0/18.0 |
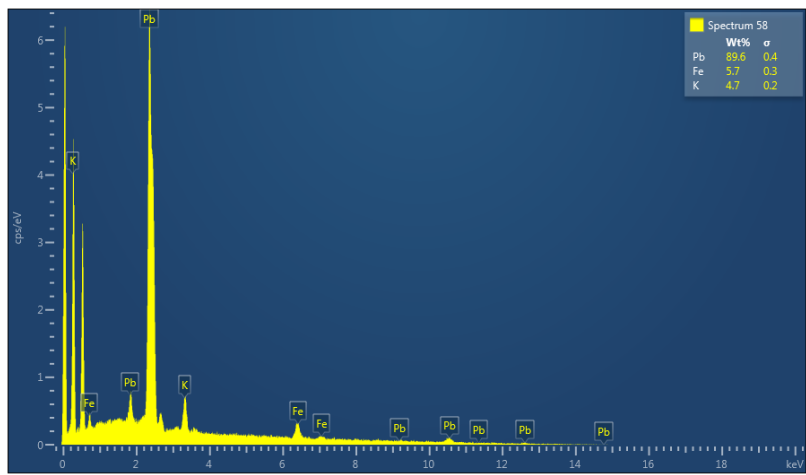


**Figure S18.** EDX analysis of **2**.

| Element | wt% | σ | Observed / Calculated Element Ratio |
|---------|------|-----|-------------------------------------|
| K | 4.7 | 0.2 | 5.0/4.0 |
| Fe | 5.7 | 0.3 | 4.2/4.0 |
| Pb | 89.6 | 0.4 | 18.0/18.0 |

14

**5. Magnetometry using the Superconducting Quantum Interference Device (SQUID)**
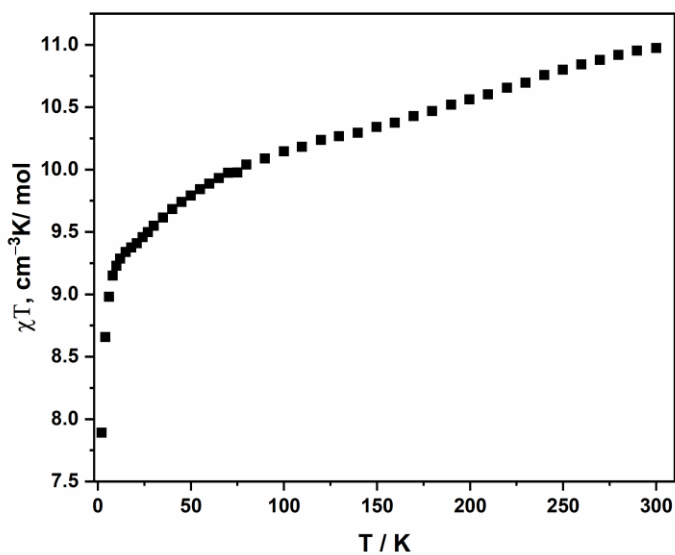


**Figure S19.** Temperature-dependent SQUID magnetometry data for **1** measured over the temperature range of 1.8 to 300 K.
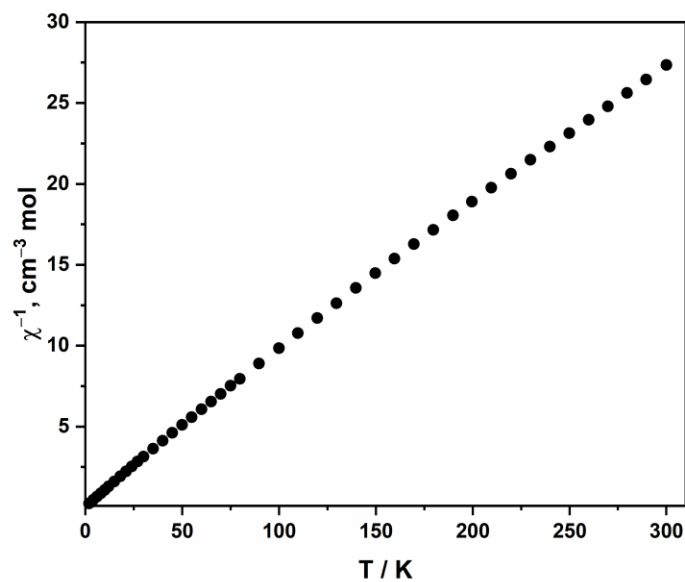


**Figure S20.** Temperature dependent, inverse solid state magnetic susceptibility for **1** collected under an applied field of H = 1000 Oe.

## 6. Computational Details

### Functional Dependence of Spin State Energies

In order to explore the dependence of the computed energies and geometries on functional choice, we have repeated the calculations reported in the main text (done with the M06-L functional) with a generalized gradient approximation (GGA) functional, PBE, and also its hybrid version, PBE0. The energies are summarized in Table S4 and S5. Note that we were unable to converge on the $S = 4$ or $S = 6$ states for the PBE0 functional. The PBE and M06-L functional give a broadly consistent picture of the relative energies of the two states with $S = 5$, $^{11}B_{3g}$ and $^{11}B_{1g}$. For $[Fe_4Sn_{18}]^{4-}$, the $^{11}B_{1g}$ state is the most stable, but the gap to the $^{11}B_{3g}$ alternative is even smaller for PBE (0.02 eV) than for M06-L (0.05 eV). This trend goes further with the PBE0 functional, where the $^{11}B_{3g}$ state is now more stable than $^{11}B_{1g}$ by 0.07 eV. The states with $S = 4$ and $S = 6$ are considerably less stable than those with $S = 5$ for both M06-L and PBE, but the latter tends to stabilize the $S = 4$ state and destabilize $S = 6$, relative to the two states with $S = 5$. Similar patterns are apparent for $[Fe_4Pb_{18}]^{4-}$, in Table S5, where the PBE functional stabilizes $^{11}B_{3g}$ relative to $^{11}B_{1g}$, although the latter is clearly more stable. PBE also stabilizes $S = 4$ and destabilizes $S = 6$ relative to the two $S = 5$ states, but the $S = 5$ remains clearly more stable. Thus, whilst there is considerable fluctuation in the relative energies, the conclusion that the $S = 5$ state is the best candidate for the ground state of both $Fe_4$ clusters appears robust.

**Table S4.** Bond energies of different spin states of $[Fe_4Sn_{18}]^{4-}$ with M06-L, PBE,[5] PBE0[6-7] functionals. All energies are in eV.

|  | S=4 | S=5 ($^{11}B_{3g}$) | S=5 ($^{11}B_{1g}$) | S=6 |
|---|---|---|---|---|
| M06-L | -121.6021 ($^9A_g$) | -122.1392 | -122.1927 | -121.9378 ($^{13}B_{2g}$) |
| PBE | -112.5093 ($^9B_{1u}$) | -112.6542 | -112.6735 | -112.2424 ($^{13}B_{3g}$) |
| PBE0 |  | - 151.1726 | - 151.0985 |  |

**Table S5.** Bond energies of different spin states of $[Fe_4Pb_{18}]^{4-}$ with M06-L and PBE functionals. All energies are in eV.

|  | S=4 ($^9B_{2u}$) | S=5 ($^{11}B_{3g}$) | S=5 ($^{11}B_{1g}$) | S=6 ($^{13}B_{3g}$) |
|---|---|---|---|---|
| M06-L | -116.0026 | -116.6095 | -116.7923 | -116.6074 |
| PBE | -106.1882 | -106.3245 | -106.4770 | -106.0472 |

### Discussion of the charge state of the E$_{18}$ cage

In our recent paper discussing the structure and properties of $[Fe_3Sn_{18}]^{4-}$,[8] we argued that the presence of partially fused $Sn_9$ polyhedra was indicative of a $Sn_{18}^{6-}$ charge state. This contrasts with the situation in $[Cd(NiSn_9)_2]^{6-}$,[9] where the two polyhedral are completely separated with a charge of 8- and also with the completely fused limit found in $[Pd_2Sn_{18}]^{4-}$,[10] where the charge is 4-. Lin and co-workers have also explored the fusion of $Sn_9$ units using their principal interacting orbitals (PIO) approach.[11,12,13] The question that we address here is which charge state is appropriate to the E$_{18}$ units in the $[Fe_4Sn_{18}]^{4-}$ and $[Fe_4Pb_{18}]^{4-}$ clusters discussed in this paper. The

stability of the Cu analogues, $[Cu_4Sn_{18}]^{4-}$ and $[Cu_4Pb_{18}]^{4-}$, where the Cu ions are unambiguously in the +1 charge state (as judged by the filled 3d band in the projected density of states plots) provides strong circumstantial evidence for the presence of an $[E_{18}]^{8-}$ unit to balance the charge.[14] We can reinforce this argument by extracting the $Sn_{18}$ units from converged geometries for $[Fe_4Sn_{18}]^{4-}$, $[Cd(NiSn_9)_2]^{6-}$ and $[Pd_2Sn_{18}]^{4-}$ and performing single point calculations on each structure in the 4- and 8- charge states (see Table S6). At the 4- charge level, it is clear that the fused geometry of the $[Pd_2Sn_{18}]^{4-}$ cluster is optimal. At the 8- charge state, the geometries obtained from $[Fe_4Sn_{18}]^{4-}$ and $[Cd(NiSn_9)_2]^{6-}$ are both more stable than that from $[Pd_2Sn_{18}]^{4-}$. The different number of metal ions in $[Fe_4Sn_{18}]^{4-}$ and $[Cd(NiSn_9)_2]^{6-}$ makes it difficult to make a direct energetic comparison, but it is clear that the geometry of the $Sn_{18}$ cluster in the former is in some sense adapted to an 80-electron count ($[Sn_{18}]^{8-}$).

**Table S6.** Bond energies of charged $Sn_{18}$ from the optimized endohedral $Sn_{18}$-based clusters. All energies are in eV.

| Charge State | Cage from $[Pd_2Sn_{18}]^{4-}$/eV | Cage from $[Cd(NiSn_9)_2]^{6-}$/eV | Cage from $[Fe_4Sn_{18}]^{4-}$/eV |
|---|---|---|---|
| 4– | -77.24 | -76.39 | -75.26 |
| 8– | -82.71 | -87.29 | -84.11 |

To develop this idea further, we have extended the analysis in our recent paper on $[Fe_3Sn_{18}]^{4-}$ using the Walsh diagram approach applied in our recent work on $[Fe_3Sn_{18}]^{4-}$, where we showed that the coalescence of the $E_9$ polyhedra across the series $[Cd(NiSn_9)_2]^{6-}$, $[Fe_3Sn_{18}]^{4-}$, $[Pd_2Sn_{18}]^{4-}$ causes the destabilisation of two orbitals, and hence a reduction in characteristic charge from 8- to 4- (Figure S21). It is not immediately obvious how to link the structure with two separated $Sn_9$ units to the fused $D_{2h}$-symmetric geometry found in $[Fe_4Sn_{18}]^{4-}$, but this can be achieved using the $D_{3d}$-symmetric $[Fe_3Sn_{18}]^{4-}$ as an intermediate, as shown in the Walsh diagram below. The first step, the partial fusion of two $Sn_9$ units, results in the destabilisation of <u>one</u> orbital and hence a reduction in characteristic charge from 8- to 6-. The second step, converting the structure found in $[Fe_3Sn_{18}]^{4-}$ to that found in $[Fe_4Sn_{18}]^{4-}$ involves a rotation of the atoms in the central $Sn_6$ unit, and results in the net stabilisation of <u>two</u> orbitals ($7b_{1u}$ and $5b_{2g}$) and the destabilisation of <u>one</u> ($9a_g$), restoring the characteristic 8- charge. In this light, we see that the separated $E_9$ limit and the $D_{2h}$-symmetric isomers of $E_{18}$ are both adapted to accommodate an electron count of precisely 80, and hence a net 8- charge, albeit in different ways: the balance between the two forms will then be determined by the availability of the metal cations.
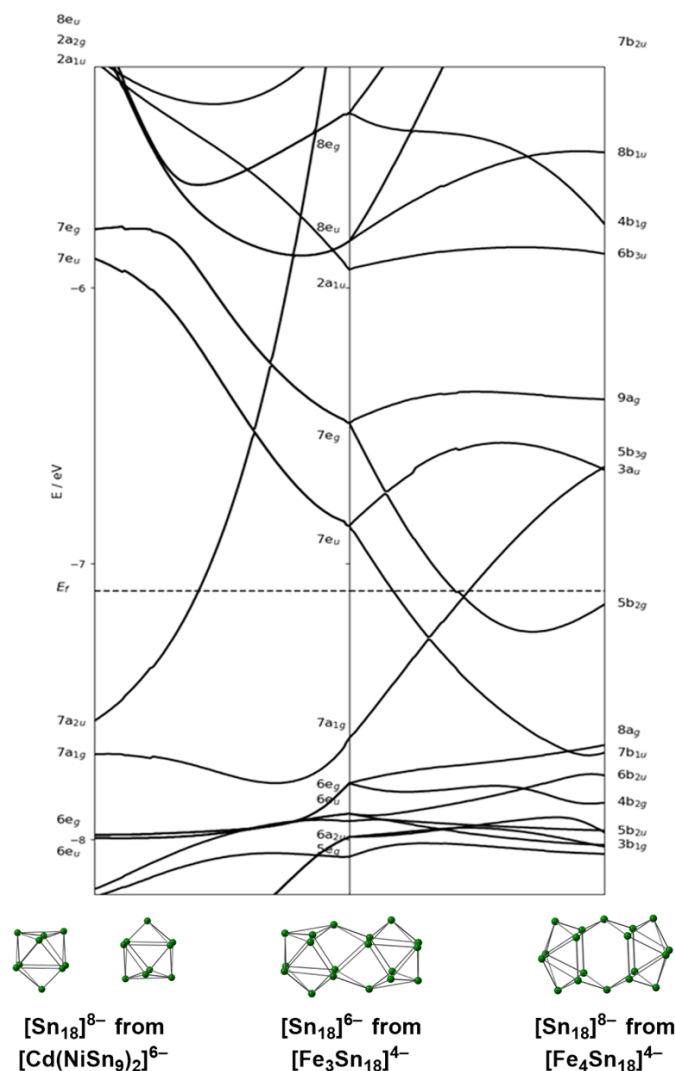
**Figure S21.** The Walsh diagram connecting three $Sn_{18}$ clusters - the separated $[Sn_{18}]^{8-}$ from optimized $[Cd(NiSn_9)_2]^{6-}$, partially fused $[Sn_{18}]^{6-}$ from optimized $[Fe_3Sn_{18}]^{4-}$ and fused $[Sn_{18}]^{8-}$ from optimized $[Fe_4Sn_{18}]^{4-}$. The orbitals vary with the geometry changes, possessing 40, 38 and 40 low-lying orbitals for three $Sn_{18}$ cages respectively.

## Electronic structure analysis using DOS, PDOS and OPDOS

The description of the bonding presented in the main text is based on a careful analysis of the Kohn-Sham orbitals and also the densities of states (DOS), projected densities of states (PDOS) and overlap-projected densities of states (OPDOS) shown in Figure S22. The eigenvalue spectrum of these molecular clusters is, of course, discrete, so a brief comment on why we adopt an analysis based on levels broadened into a density of states using an arbitrary Lorentzian line width is in order. The PDOS defines the contribution of different atomic levels to the DOS at a given energy while the OPDOS, sometimes referred to at the Crystal Orbital Overlap Population (COOP) in a solid-state context, defines the degree of bonding (positive) or antibonding (negative) character for a given atom pair as a function of energy. The trio of DOS, PDOS and OPDOS provide

18

a graphical picture of (a) the energies of the orbitals, (b) their composition (PDOS) and (c) their bonding/antibonding character (OPDOS). It therefore allows for a rapid assessment of, for example, the degree of Fe-Fe bonding character in a given configuration. The PDOS in Figure S23 is projected onto Fe/Cu 3d and Sn 5p/Pb 6p states while the OPDOS is projected onto the M1-M2 and M2-M2′ pairs (only the spin-β manifolds are shown for the latter). As discussed in our previous paper, the PDOS of the Cu cluster is highly characteristic of closed-shell $Cu^+$: a narrow occupied band of Cu 3d levels between −3 and −4 eV (relative to the Fermi level) contains all Cu-Cu linear combinations from bonding (positive OPDOS) to antibonding (negative OPDOS). The band of Sn 5p or Pb 6p levels lies above Cu 3d, between −3 eV and the Fermi level, and there is limited mixing of Cu and tetrel levels: the interaction between Cu and Sn can be considered, to a good first approximation, as an ionic one. The assignment of an oxidation state to Fe in $[Fe_4Sn_{18}]^{4-}$ and $[Fe_4Pb_{18}]^{4-}$ is less straightforward, but the striking similarities between the Sn 5p PDOS of $[Cu_4Sn_{18}]^{4-}$ and $[Fe_4Sn_{18}]^{4-}$ is a first indication that the $E_{18}$ units share a common oxidation level and so, therefore, must the transition metal ions (*i.e.* $Cu_4^{4+}$ and $Fe_4^{4+}$). The OPDOS shows that the doubly-occupied levels are largely Fe1-Fe2 (blue OPDOS curve) and Fe2-Fe2′ (red OPDOS curve) bonding while the singly-occupied and vacant levels are largely antibonding, and the excess of bonding over antibonding electrons gives rise to net Fe-Fe bonding. We can identify three distinct bonding/antibonding orbital pairs that make a substantial net contributions to the Fe2-Fe2′ bonding in both the $^{11}B_{1g}$ and $^{11}B_{3g}$ states: the $8a_g^2 8b_{2u}^1$ configuration (Fe2-Fe2′ σ), the $4b_{1u}^2 5b_{3g}^1$ configuration (out-of-plane π) and the $7b_{3u}^2 7b_{1g}^0$ configuration (in-plane π). The dominant peaks in the Fe1-Fe2 OPDOS, in contrast, come from the $5b_{2g}^2 4a_u^1$ configuration (out-of-plane π). The differences between the $^{11}B_{3g}$ and $^{11}B_{1g}$ states then lie in the reversal of the $6b_{1g}$ and $4b_{3g}$ orbitals, the first of which has significant Fe2-Fe2′ in-plane $\pi^*$ character (negative OPDOS): the strengthening of this in-plane component in the $^{11}B_{1g}$ state is responsible for the contraction of the Fe2-Fe2′ bond in $[Fe_4Pb_{18}]^{4-}$. The differences between Cu and Fe, and between Sn and Pb, are captured in Table 2, where the bond lengths, Mayer bond orders (MBO), and delocalization indices (DI), both of which correlate with bond strength, are collected. The values for the Cu clusters again establish a baseline corresponding to weak interactions of a cuprophilic type. The Mayer bond orders and delocalization indices are systematically larger for the Fe-Fe bonds compared to their Cu-Cu counterparts, with the most striking differences coming in the $^{11}B_{1g}$ states, where the Fe2-Fe2′ bonds have bond orders greater than 0.8 compared to values of ~0.6 in the $^{11}B_{3g}$ state. The contraction of the Fe2-Fe2′ bond in $[Fe_4Pb_{18}]^{4-}$ compared to $[Fe_4Sn_{18}]^{4-}$ appears, therefore, to mark a very substantial increase in π component of the bond.
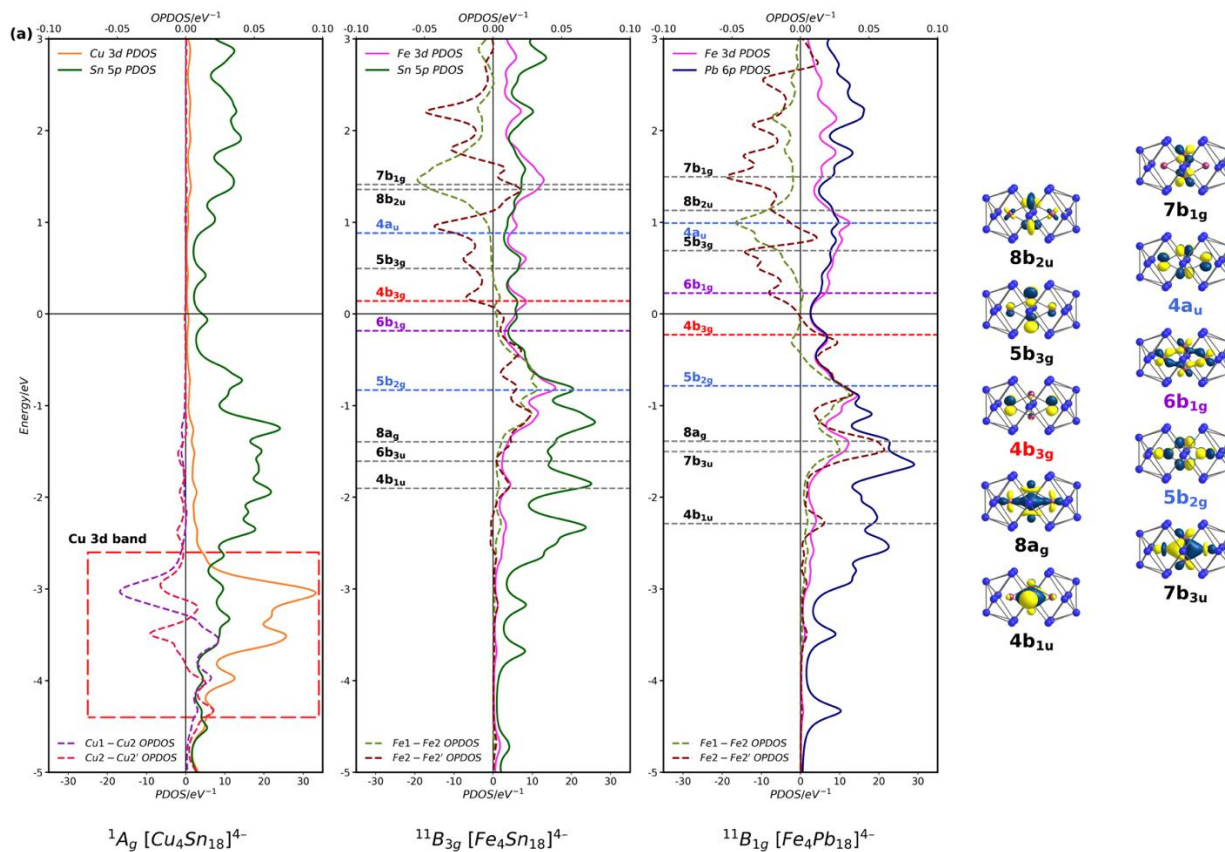
**Figure S22.** The PDOS and OPDOS for $[Cu_4Sn_{18}]^{4-}$, and for the spin-b manifolds of $[Fe_4Sn_{18}]^{4-}$ and $[Fe_4Pb_{18}]^{4-}$. The two spin components, α and β, of the PDOS and OPDOS for $[Fe_4Sn_{18}]^{4-}$ and $[Fe_4Pb_{18}]^{4-}$ are collected in Figures S22 and S23 (only the spin-β components are shown in Figure S22). In both cases, the Fe-Fe antibonding orbitals lie largely above the Fermi level in the spin-β set, but below it in spin-α. This leads to an accumulation of bonding character.
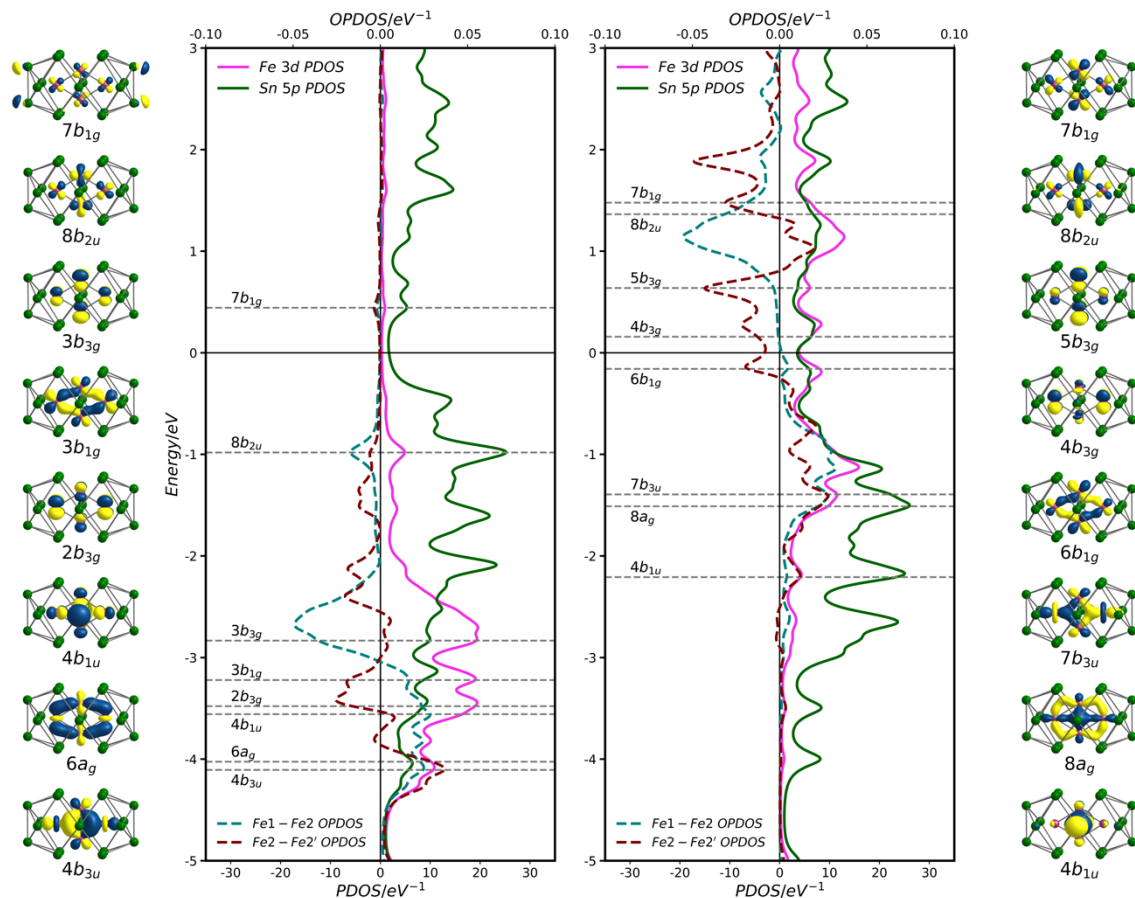
**Figure S23.** The PDOS and OPDOS for both majority and minority spin of $[Fe_4Sn_{18}]^{4-}$. The energy levels that mediate the σ and π contributions to Fe2-Fe2' bonds are labelled, as are the two orbitals that switch occupancies between the $^{11}B_{1g}$ and $^{11}B_{3g}$ states.
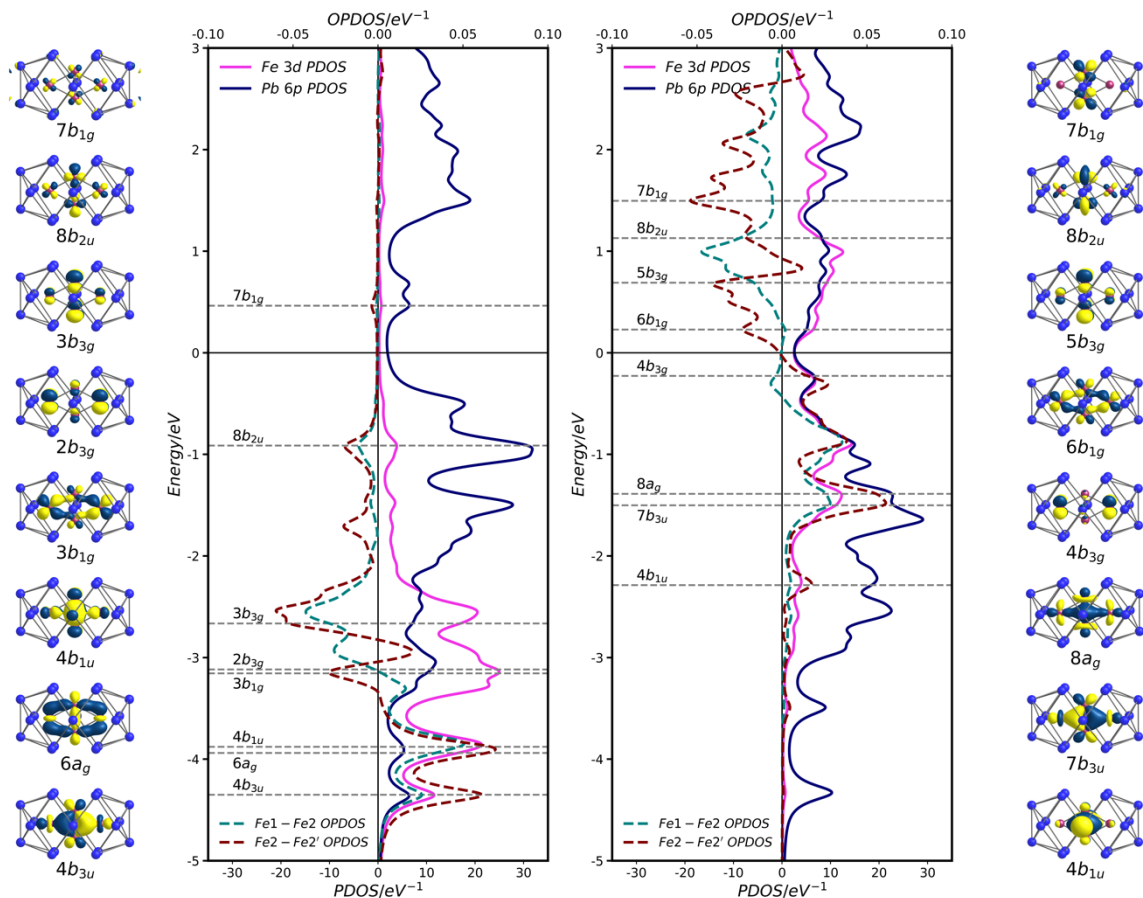
**Figure S24.** The PDOS and OPDOS for both majority and minority spin of $[Fe_4Pb_{18}]^{4-}$. The energy levels that mediate the σ and π contributions to Fe2-Fe2' bonds are labelled, as are the two orbitals that switch occupancies between the $^{11}B_{1g}$ and $^{11}B_{3g}$ states.

Electron Localization Functions (ELF) and density distribution analysis

The emergence of Fe-Fe bonding is also illustrated graphically by the electron density distributions in Figure S25 and the electron localization functions (ELF), shown in Figure S26. The accumulation of density at the mid-point of the Fe1-Fe2 and Fe2-Fe2' vectors in both $[Fe_4Sn_{18}]^{4-}$ and $[Fe_4Pb_{18}]^{4-}$ is clear, as is the positive (orange and red) ELF basin along the Fe1-Fe2 vectors and in the center of $Fe_4$ rhombus.
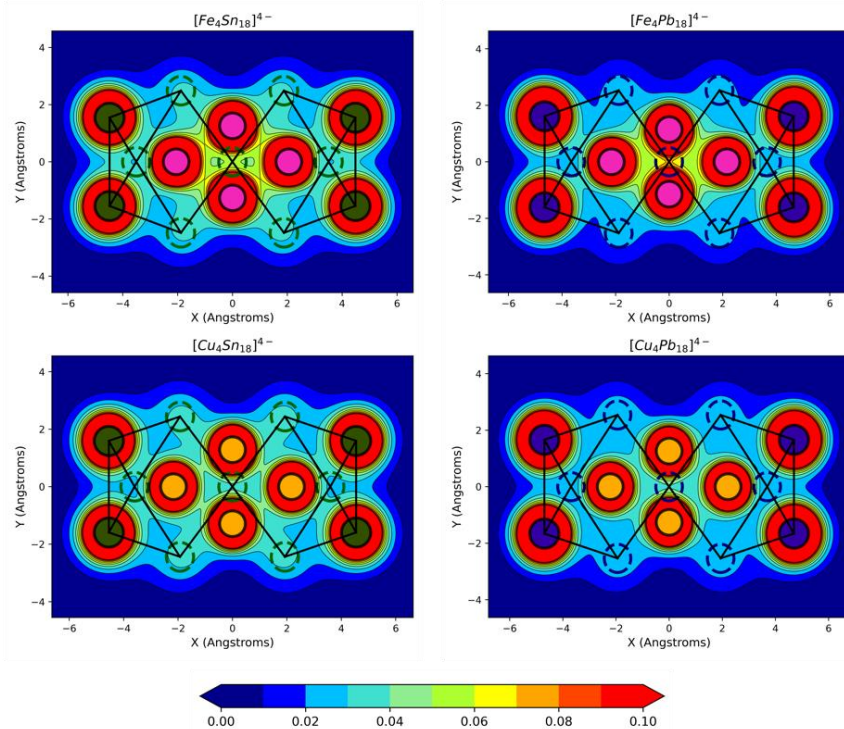
**Figure S25.** Electron density distributions of $[Fe_4E_{18}]^{4-}$ and $[Cu_4E_{18}]^{4-}$ (E = Sn, Pb) on the $M_4$ planes. The density increases with the color from blue to red. The contour range is 0 to 0.1.
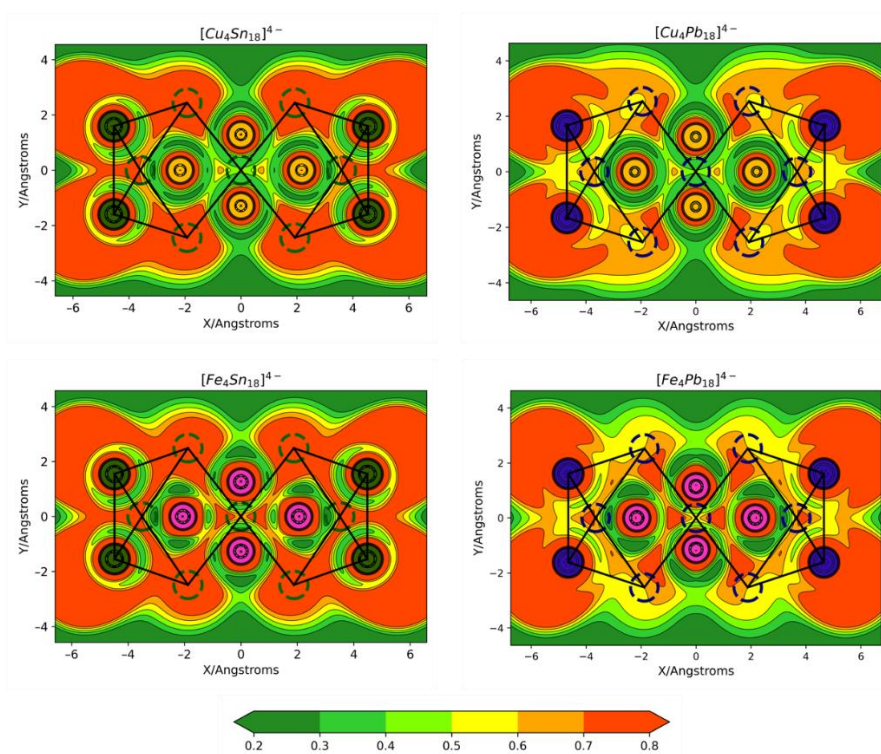


**Figure S26.** Electron localization functions (ELF) for $[Cu_4E_{18}]^{4-}$ and $[Fe_4E_{18}]^{4-}$ and on the $M_4$ planes. The contour range is from 0.2 to 0.8.

23

**Table S7.** Mayer bond orders (MBO), delocalisation indices (DI) and ellipticities ($\varepsilon$) of the Fe-Fe bond critical points.

| | | | M-M | MBO | DI | $\varepsilon$ |
|---|---|---|---|---|---|---|
| $[Fe_4Sn_{18}]^{4-}$ | $^{11}B_{1g}$ | Fe1-Fe2 | 2.42 | 0.82 | 0.68 | 0.91 |
| | | Fe2-Fe2' | 2.31 | 0.82 | 0.97 | 0.45 |
| | $^{11}B_{3g}$ | Fe1-Fe2 | 2.41 | 0.85 | 0.74 | 0.26 |
| | | Fe2-Fe2' | 2.52 | 0.51 | 0.64 | 2.11 |
| $[Fe_4Pb_{18}]^{4-}$ | $^{11}B_{1g}$ | Fe1-Fe2 | 2.44 | 0.69 | 0.70 | 1.02 |
| | | Fe2-Fe2' | 2.28 | 0.91 | 1.00 | 0.46 |
| | $^{11}B_{3g}$ | Fe1-Fe2 | 2.43 | 0.74 | 0.75 | 0.31 |
| | | Fe2-Fe2' | 2.48 | 0.62 | 0.70 | 1.77 |
| $[Cu_4Sn_{18}]^{4-}$ | $^{1}A_{g}$ | Cu1-Cu2 | 2.52 | 0.41 | 0.32 | 0.20 |
| | | Cu2-Cu2' | 2.58 | 0.10 | 0.29 | 0.15 |
| $[Cu_4Pb_{18}]^{4-}$ | $^{1}A_{g}$ | Cu1-Cu2 | 2.55 | 0.31 | 0.32 | 0.23 |
| | | Cu2-Cu2' | 2.52 | 0.18 | 0.32 | 0.22 |

**Coordinates of Computational Results (Appendix)**

The optimized cartesian coordinates of the corresponding stationary points of $^{11}B_{1g}$ and $^{11}B_{3g}$ states of $[Fe_4Sn_{18}]^{4-}$ and $[Fe_4Pb_{18}]^{4-}$, with bond energies provided.

***D*$_{2h}$-[Fe$_4$Sn$_{18}$]$^{4-}$ ($^{11}B_{1g}$) M06-L**; S = 5; Bond Energy = -122.1927 eV
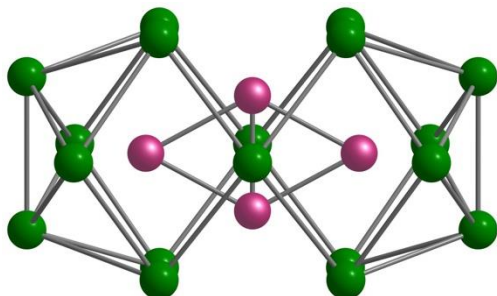


| Fe | -2.130715 | -0.000000 | 0.000000 |
|----|-----------|-----------|----------|
| Fe | -0.000000 | 1.153535 | 0.000000 |
| Fe | 0.000000 | -1.153535 | 0.000000 |
| Fe | 2.130715 | 0.000000 | 0.000000 |
| Sn | -4.507484 | -1.532943 | 0.000000 |
| Sn | -4.507484 | 1.532943 | 0.000000 |
| Sn | -3.561771 | 0.000000 | -2.521662 |
| Sn | -3.561771 | 0.000000 | 2.521662 |
| Sn | -1.861710 | -2.409333 | -1.579990 |
| Sn | -1.861710 | -2.409333 | 1.579990 |
| Sn | -1.861710 | 2.409333 | -1.579990 |
| Sn | -1.861710 | 2.409333 | 1.579990 |
| Sn | 0.000000 | -0.000000 | -2.536886 |
| Sn | 0.000000 | 0.000000 | 2.536886 |
| Sn | 1.861710 | -2.409333 | -1.579990 |
| Sn | 1.861710 | -2.409333 | 1.579990 |
| Sn | 1.861710 | 2.409333 | -1.579990 |
| Sn | 1.861710 | 2.409333 | 1.579990 |
| Sn | 3.561771 | -0.000000 | -2.521662 |
| Sn | 3.561771 | -0.000000 | 2.521662 |
| Sn | 4.507484 | -1.532943 | 0.000000 |
| Sn | 4.507484 | 1.532943 | 0.000000 |

***D*$_{2h}$-[Fe$_4$Sn$_{18}$]$^{4-}$ ($^{11}B_{3g}$) M06-L**; S = 5; Bond Energy = -122.1392 eV
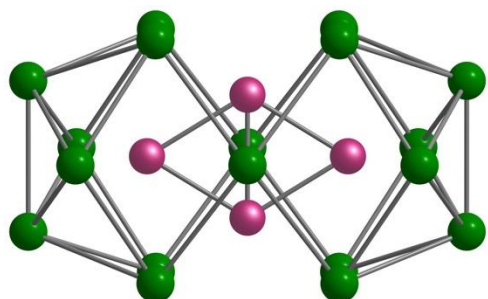
| Fe | -2.054520 | -0.000000 | 0.000000 |
|----|-----------|-----------|----------|
| Fe | -0.000000 | 1.259551 | 0.000000 |
| Fe | 0.000000 | -1.259551 | 0.000000 |
| Fe | 2.054520 | 0.000000 | 0.000000 |
| Sn | -4.481842 | -1.545122 | 0.000000 |
| Sn | -4.481842 | 1.545122 | 0.000000 |
| Sn | -3.506483 | 0.000000 | -2.482056 |
| Sn | -3.506483 | 0.000000 | 2.482056 |
| Sn | -1.877336 | -2.486922 | -1.545396 |
| Sn | -1.877336 | -2.486922 | 1.545396 |
| Sn | -1.877336 | 2.486922 | -1.545396 |
| Sn | -1.877336 | 2.486922 | 1.545396 |
| Sn | 0.000000 | -0.000000 | 2.443174 |
| Sn | 0.000000 | 0.000000 | -2.443174 |
| Sn | 1.877336 | -2.486922 | -1.545396 |
| Sn | 1.877336 | -2.486922 | 1.545396 |
| Sn | 1.877336 | 2.486922 | -1.545396 |
| Sn | 1.877336 | 2.486922 | 1.545396 |
| Sn | 3.506483 | -0.000000 | -2.482056 |
| Sn | 3.506483 | -0.000000 | 2.482056 |
| Sn | 4.481842 | -1.545122 | 0.000000 |
| Sn | 4.481842 | 1.545122 | 0.000000 |

*D$_{2h}$*-[Fe$_4$Pb$_{18}$]$^{4-}$ ($^{11}$B$_{1g}$) **M06-L**; S = 5; Bond Energy = -116.7924 eV
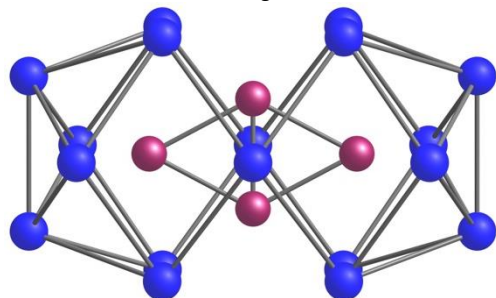


| Fe | -2.155771 | 0.000000 | 0.000000 |
|----|-----------|----------|----------|
| Fe | 0.000000 | -1.142377 | 0.000000 |
| Fe | 0.000000 | 1.142377 | 0.000000 |
| Fe | 2.155771 | 0.000000 | 0.000000 |

| Pb | -4.653745 | -1.611333 | 0.000000 |
|----|-----------|-----------|----------|
| Pb | -4.653745 | 1.611333 | 0.000000 |
| Pb | -3.656158 | 0.000000 | -2.630213 |
| Pb | -3.656158 | 0.000000 | 2.630213 |
| Pb | -1.882569 | -2.527431 | -1.637573 |
| Pb | -1.882569 | -2.527431 | 1.637573 |
| Pb | -1.882569 | 2.527431 | -1.637573 |
| Pb | -1.882569 | 2.527431 | 1.637573 |
| Pb | 0.000000 | 0.000000 | -2.667369 |
| Pb | 0.000000 | 0.000000 | 2.667369 |
| Pb | 1.882569 | -2.527431 | -1.637573 |
| Pb | 1.882569 | -2.527431 | 1.637573 |
| Pb | 1.882569 | 2.527431 | -1.637573 |
| Pb | 1.882569 | 2.527431 | 1.637573 |
| Pb | 3.656158 | 0.000000 | -2.630213 |
| Pb | 3.656158 | 0.000000 | 2.630213 |
| Pb | 4.653745 | -1.611333 | 0.000000 |
| Pb | 4.653745 | 1.611333 | 0.000000 |

**$D_{2h}$-[Fe$_4$Pb$_{18}$]$^{4-}$ ($^{11}$B$_{3g}$) M06-L**; S = 5; Bond Energy = -116.6095 eV
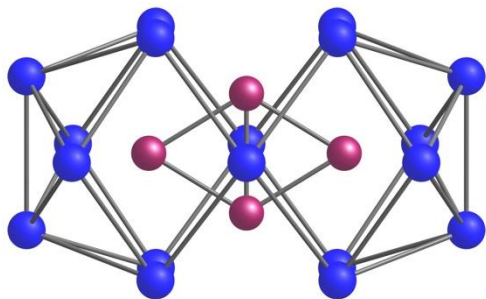


| Fe | -2.086286 | 0.000000 | 0.000000 |
|----|-----------|-----------|----------|
| Fe | 0.000000 | -1.237961 | 0.000000 |
| Fe | 0.000000 | 1.237961 | 0.000000 |
| Fe | 2.086286 | 0.000000 | 0.000000 |
| Pb | -4.628587 | -1.626312 | 0.000000 |
| Pb | -4.628587 | 1.626312 | 0.000000 |
| Pb | -3.601909 | 0.000000 | -2.591589 |
| Pb | -3.601909 | 0.000000 | 2.591589 |
| Pb | -1.895771 | -2.603710 | -1.613053 |
| Pb | -1.895771 | -2.603710 | 1.613053 |
| Pb | -1.895771 | 2.603710 | -1.613053 |
| Pb | -1.895771 | 2.603710 | 1.613053 |
| Pb | 0.000000 | 0.000000 | -2.582918 |
| Pb | 0.000000 | 0.000000 | 2.582918 |
| Pb | 1.895771 | -2.603710 | -1.613053 |
| Pb | 1.895771 | -2.603710 | 1.613053 |

| Pb | 1.895771 | 2.603710 | -1.613053 |
|----|----------|----------|-----------|
| Pb | 1.895771 | 2.603710 | 1.613053 |
| Pb | 3.601909 | 0.000000 | -2.591589 |
| Pb | 3.601909 | 0.000000 | 2.591589 |
| Pb | 4.628587 | -1.626312 | 0.000000 |
| Pb | 4.628587 | 1.626312 | 0.000000 |

The optimized cartesian coordinates of 9et and 13et of $[Fe_4Sn_{18}]^{4-}$ and $[Fe_4Pb_{18}]^{4-}$, with bond energies provided. Stationary points were confirmed.

$D_{2h}$-$[Fe_4Sn_{18}]^{4-}$ ($^9A_g$) M06-L; S = 4; Bond Energy = -121.6021 eV
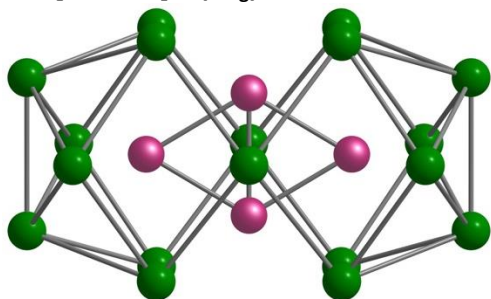


| Fe | -2.070819 | -0.000000 | 0.000000 |
|----|-----------|-----------|----------|
| Fe | -0.000000 | -1.236232 | 0.000000 |
| Fe | 0.000000 | 1.236232 | 0.000000 |
| Fe | 2.070819 | 0.000000 | 0.000000 |
| Sn | -4.474137 | -1.547014 | 0.000000 |
| Sn | -4.474137 | 1.547014 | 0.000000 |
| Sn | -3.540801 | 0.000000 | -2.503259 |
| Sn | -3.540801 | 0.000000 | 2.503259 |
| Sn | -1.866031 | -2.416192 | -1.581613 |
| Sn | -1.866031 | -2.416192 | 1.581613 |
| Sn | -1.866031 | 2.416192 | -1.581613 |
| Sn | -1.866031 | 2.416192 | 1.581613 |
| Sn | 0.000000 | -0.000000 | -2.457478 |
| Sn | 0.000000 | 0.000000 | 2.457478 |
| Sn | 1.866031 | -2.416192 | -1.581613 |
| Sn | 1.866031 | -2.416192 | 1.581613 |
| Sn | 1.866031 | 2.416192 | -1.581613 |
| Sn | 1.866031 | 2.416192 | 1.581613 |
| Sn | 3.540801 | -0.000000 | -2.503259 |
| Sn | 3.540801 | -0.000000 | 2.503259 |
| Sn | 4.474137 | -1.547014 | 0.000000 |
| Sn | 4.474137 | 1.547014 | 0.000000 |

$D_{2h}$-$[Fe_4Sn_{18}]^{4-}$ ($^{13}B_{2g}$) M06-L; S = 6; Bond Energy = -121.9378 eV
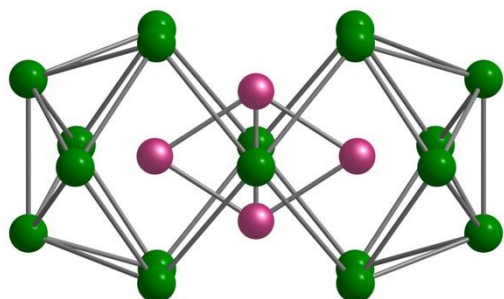
| Fe | -2.042279 | -0.000000 | 0.000000 |
|----|-----------|-----------|----------|
| Fe | -0.000000 | 1.314034 | 0.000000 |
| Fe | 0.000000 | -1.314034 | 0.000000 |
| Fe | 2.042279 | 0.000000 | 0.000000 |
| Sn | -4.595467 | -1.562767 | 0.000000 |
| Sn | -4.595467 | 1.562767 | 0.000000 |
| Sn | -3.637559 | -0.000000 | -2.477535 |
| Sn | -3.637559 | -0.000000 | 2.477535 |
| Sn | -2.004794 | -2.431050 | -1.543943 |
| Sn | -2.004794 | -2.431050 | 1.543943 |
| Sn | -2.004794 | 2.431050 | -1.543943 |
| Sn | -2.004794 | 2.431050 | 1.543943 |
| Sn | 0.000000 | -0.000000 | 2.420789 |
| Sn | 0.000000 | 0.000000 | -2.420789 |
| Sn | 2.004794 | -2.431050 | -1.543943 |
| Sn | 2.004794 | -2.431050 | 1.543943 |
| Sn | 2.004794 | 2.431050 | -1.543943 |
| Sn | 2.004794 | 2.431050 | 1.543943 |
| Sn | 3.637559 | 0.000000 | -2.477535 |
| Sn | 3.637559 | 0.000000 | 2.477535 |
| Sn | 4.595467 | -1.562767 | 0.000000 |
| Sn | 4.595467 | 1.562767 | 0.000000 |

*D2h*-[Fe₄Pb₁₈]⁴⁻ (⁹B₁ᵤ) M06-L; S = 4; Bond Energy = -116.0026 eV

$D_{2h}$-[Fe$_4$Pb$_{18}$]$^{4-}$ ($^9$B$_{1u}$) M06-L; S = 4; Bond Energy = -116.0026 eV
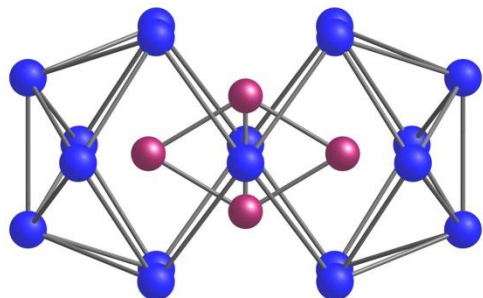


| Fe | -2.069987 | -0.000000 | 0.000000 |
|----|-----------|-----------|----------|
| Fe | 0.000000 | -1.230955 | 0.000000 |
| Fe | 0.000000 | 1.230955 | -0.000000 |
| Fe | 2.069987 | 0.000000 | 0.000000 |

| Pb | -4.632883 | -1.616400 | 0.000000 |
| Pb | -4.632883 | 1.616400 | -0.000000 |
| Pb | -3.555866 | -0.000000 | 2.597529 |
| Pb | -3.555866 | 0.000000 | -2.597529 |
| Pb | -1.903795 | -2.594250 | -1.614491 |
| Pb | -1.903795 | -2.594250 | 1.614491 |
| Pb | -1.903795 | 2.594250 | -1.614491 |
| Pb | -1.903795 | 2.594250 | 1.614491 |
| Pb | 0.000000 | -0.000000 | 2.628148 |
| Pb | 0.000000 | 0.000000 | -2.628148 |
| Pb | 1.903795 | -2.594250 | -1.614491 |
| Pb | 1.903795 | -2.594250 | 1.614491 |
| Pb | 1.903795 | 2.594250 | -1.614491 |
| Pb | 1.903795 | 2.594250 | 1.614491 |
| Pb | 3.555866 | -0.000000 | 2.597529 |
| Pb | 3.555866 | 0.000000 | -2.597529 |
| Pb | 4.632883 | -1.616400 | 0.000000 |
| Pb | 4.632883 | 1.616400 | -0.000000 |

**$D_{2h}$-[Fe$_4$Pb$_{18}$]$^{4-}$ ($^{13}$B$_{3g}$) M06-L**; S = 6; Bond Energy = -116.6074 eV
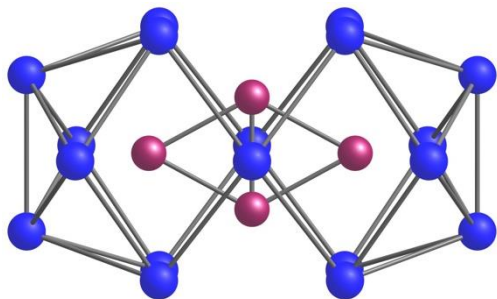


| Fe | -2.161117 | 0.000000 | 0.000000 |
| Fe | 0.000000 | -1.175322 | 0.000000 |
| Fe | 0.000000 | 1.175322 | -0.000000 |
| Fe | 2.161117 | -0.000000 | 0.000000 |
| Pb | -4.719939 | -1.640677 | 0.000000 |
| Pb | -4.719939 | 1.640677 | -0.000000 |
| Pb | -3.690727 | -0.000000 | 2.592842 |
| Pb | -3.690727 | 0.000000 | -2.592842 |
| Pb | -1.944816 | -2.560814 | -1.612833 |
| Pb | -1.944816 | -2.560814 | 1.612833 |
| Pb | -1.944816 | 2.560814 | -1.612833 |
| Pb | -1.944816 | 2.560814 | 1.612833 |
| Pb | 0.000000 | -0.000000 | 2.602707 |
| Pb | 0.000000 | 0.000000 | -2.602707 |
| Pb | 1.944816 | -2.560814 | -1.612833 |
| Pb | 1.944816 | -2.560814 | 1.612833 |

| Pb | 1.944816 | 2.560814 | -1.612833 |
| Pb | 1.944816 | 2.560814 | 1.612833 |
| Pb | 3.690727 | -0.000000 | 2.592842 |
| Pb | 3.690727 | 0.000000 | -2.592842 |
| Pb | 4.719939 | -1.640677 | 0.000000 |
| Pb | 4.719939 | 1.640677 | -0.000000 |

**The optimized coordinates of $[Fe_4Sn_{18}]^{4-}$ and $[Fe_4Pb_{18}]^{4-}$ under other functionals (PBE and PBE0), with corresponding bond energies. Stationary points were confirmed.**

*$D_{2h}$*-$[Fe_4Sn_{18}]^{4-}$ ($^{11}B_{1g}$) **PBE**; S = 5; Bond Energy = -112.6735 eV
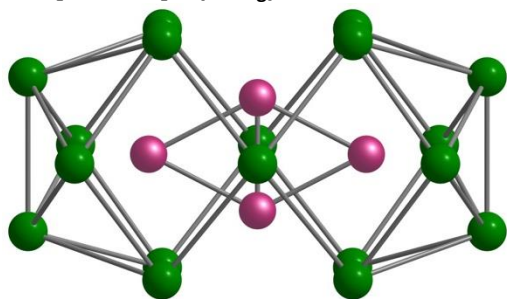


| Fe | -2.154070 | -0.000000 | 0.000000 |
| Fe | 0.000000 | -1.118983 | -0.000000 |
| Fe | 0.000000 | 1.118983 | 0.000000 |
| Fe | 2.154070 | 0.000000 | 0.000000 |
| Sn | -4.543798 | -1.531427 | 0.000000 |
| Sn | -4.543798 | 1.531427 | -0.000000 |
| Sn | -3.610798 | -0.000000 | 2.512863 |
| Sn | -3.610798 | 0.000000 | -2.512863 |
| Sn | -1.887490 | -2.369052 | -1.567209 |
| Sn | -1.887490 | -2.369052 | 1.567209 |
| Sn | -1.887490 | 2.369052 | -1.567209 |
| Sn | -1.887490 | 2.369052 | 1.567209 |
| Sn | 0.000000 | -0.000000 | -2.557180 |
| Sn | 0.000000 | 0.000000 | 2.557180 |
| Sn | 1.887490 | -2.369052 | -1.567209 |
| Sn | 1.887490 | -2.369052 | 1.567209 |
| Sn | 1.887490 | 2.369052 | -1.567209 |
| Sn | 1.887490 | 2.369052 | 1.567209 |
| Sn | 3.610798 | -0.000000 | 2.512863 |
| Sn | 3.610798 | 0.000000 | -2.512863 |
| Sn | 4.543798 | -1.531427 | 0.000000 |
| Sn | 4.543798 | 1.531427 | -0.000000 |

*$D_{2h}$*-$[Fe_4Sn_{18}]^{4-}$ ($^{11}B_{3g}$) **PBE**; S = 5; Bond Energy = -112.6542 eV
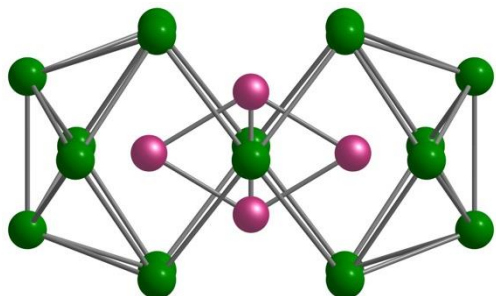
| Fe | -2.056073 | 0.000000 | 0.000000 |
| Fe | 0.000000 | -1.237769 | 0.000000 |
| Fe | 0.000000 | 1.237769 | 0.000000 |
| Fe | 2.056073 | 0.000000 | 0.000000 |
| Sn | -4.508401 | -1.546406 | 0.000000 |
| Sn | -4.508401 | 1.546406 | 0.000000 |
| Sn | -3.530526 | 0.000000 | -2.472283 |
| Sn | -3.530526 | 0.000000 | 2.472283 |
| Sn | -1.896936 | -2.457632 | -1.530740 |
| Sn | -1.896936 | -2.457632 | 1.530740 |
| Sn | -1.896936 | 2.457632 | -1.530740 |
| Sn | -1.896936 | 2.457632 | 1.530740 |
| Sn | 0.000000 | 0.000000 | -2.455217 |
| Sn | 0.000000 | 0.000000 | 2.455217 |
| Sn | 1.896936 | -2.457632 | -1.530740 |
| Sn | 1.896936 | -2.457632 | 1.530740 |
| Sn | 1.896936 | 2.457632 | -1.530740 |
| Sn | 1.896936 | 2.457632 | 1.530740 |
| Sn | 3.530526 | 0.000000 | -2.472283 |
| Sn | 3.530526 | 0.000000 | 2.472283 |
| Sn | 4.508401 | -1.546406 | 0.000000 |
| Sn | 4.508401 | 1.546406 | 0.000000 |

*D*$_{2h}$-[Fe$_4$Sn$_{18}$]$^{4-}$ (⁹B$_{2u}$) **PBE**; S = 4; Bond Energy = -112.5093 eV
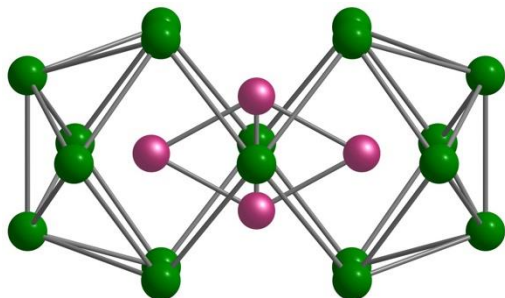


| Fe | -2.076626 | -0.000000 | 0.000000 |
| Fe | 0.000000 | -1.129888 | -0.000000 |
| Fe | 0.000000 | 1.129888 | 0.000000 |
| Fe | 2.076626 | 0.000000 | 0.000000 |

| Sn | -4.519003 | -1.538511 | -0.000000 |
| Sn | -4.519003 | 1.538511 | 0.000000 |
| Sn | -3.590976 | -0.000000 | -2.505059 |
| Sn | -3.590976 | 0.000000 | 2.505059 |
| Sn | -1.884617 | -2.376204 | -1.543629 |
| Sn | -1.884617 | -2.376204 | 1.543629 |
| Sn | -1.884617 | 2.376204 | -1.543629 |
| Sn | -1.884617 | 2.376204 | 1.543629 |
| Sn | 0.000000 | -0.000000 | -2.553677 |
| Sn | 0.000000 | 0.000000 | 2.553677 |
| Sn | 1.884617 | -2.376204 | -1.543629 |
| Sn | 1.884617 | -2.376204 | 1.543629 |
| Sn | 1.884617 | 2.376204 | -1.543629 |
| Sn | 1.884617 | 2.376204 | 1.543629 |
| Sn | 3.590976 | -0.000000 | -2.505059 |
| Sn | 3.590976 | 0.000000 | 2.505059 |
| Sn | 4.519003 | -1.538511 | -0.000000 |
| Sn | 4.519003 | 1.538511 | 0.000000 |

*D*$_{2h}$-[Fe$_4$Sn$_{18}$]$^{4-}$ ($^{13}$B$_{3g}$) PBE; S = 6; Bond Energy = -112.2424 eV
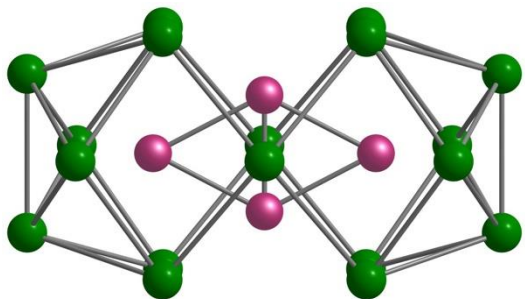


| Fe | -2.181900 | 0.000000 | 0.000000 |
| Fe | 0.000000 | -1.139100 | 0.000000 |
| Fe | 0.000000 | 1.139100 | 0.000000 |
| Fe | 2.181900 | 0.000000 | 0.000000 |
| Sn | -4.646300 | -1.556300 | 0.000000 |
| Sn | -4.646300 | 1.556300 | 0.000000 |
| Sn | -3.688000 | 0.000000 | -2.482400 |
| Sn | -3.688000 | 0.000000 | 2.482400 |
| Sn | -1.992200 | -2.373300 | -1.536400 |
| Sn | -1.992200 | -2.373300 | 1.536400 |
| Sn | -1.992200 | 2.373300 | -1.536400 |
| Sn | -1.992200 | 2.373300 | 1.536400 |
| Sn | 0.000000 | 0.000000 | -2.488500 |
| Sn | 0.000000 | 0.000000 | 2.488500 |
| Sn | 1.992200 | -2.373300 | -1.536400 |
| Sn | 1.992200 | -2.373300 | 1.536400 |

| Sn | 1.992200 | 2.373300 | -1.536400 |
| Sn | 1.992200 | 2.373300 | 1.536400 |
| Sn | 3.688000 | 0.000000 | -2.482400 |
| Sn | 3.688000 | 0.000000 | 2.482400 |
| Sn | 4.646300 | -1.556300 | 0.000000 |
| Sn | 4.646300 | 1.556300 | 0.000000 |

**$D_{2h}$-[Fe$_4$Pb$_{18}$]$^{4-}$ ($^{11}$B$_{1g}$) PBE**; S = 5; Bond Energy = -106.4770 eV
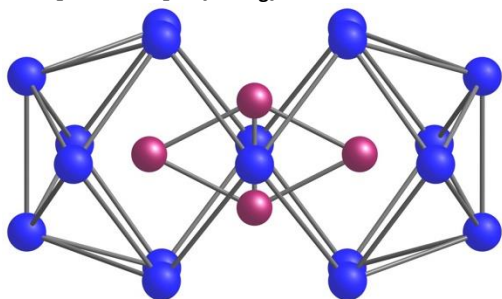


| Fe | -2.165392 | 0.000000 | 0.000000 |
| Fe | 0.000000 | -1.102186 | 0.000000 |
| Fe | 0.000000 | 1.102186 | 0.000000 |
| Fe | 2.165392 | 0.000000 | 0.000000 |
| Pb | -4.684661 | -1.602776 | 0.000000 |
| Pb | -4.684661 | 1.602776 | 0.000000 |
| Pb | -3.712302 | 0.000000 | -2.617373 |
| Pb | -3.712302 | 0.000000 | 2.617373 |
| Pb | -1.910978 | -2.475537 | -1.622707 |
| Pb | -1.910978 | -2.475537 | 1.622707 |
| Pb | -1.910978 | 2.475537 | -1.622707 |
| Pb | -1.910978 | 2.475537 | 1.622707 |
| Pb | 0.000000 | 0.000000 | -2.699830 |
| Pb | 0.000000 | 0.000000 | 2.699830 |
| Pb | 1.910978 | -2.475537 | -1.622707 |
| Pb | 1.910978 | -2.475537 | 1.622707 |
| Pb | 1.910978 | 2.475537 | -1.622707 |
| Pb | 1.910978 | 2.475537 | 1.622707 |
| Pb | 3.712302 | 0.000000 | -2.617373 |
| Pb | 3.712302 | 0.000000 | 2.617373 |
| Pb | 4.684661 | -1.602776 | 0.000000 |
| Pb | 4.684661 | 1.602776 | 0.000000 |

**$D_{2h}$-[Fe$_4$Pb$_{18}$]$^{4-}$ ($^{11}$B$_{3g}$) PBE**; S = 5; Bond Energy = - 106.3127 eV
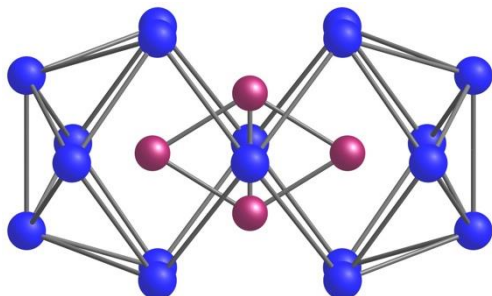
| Fe | -2.068925 | 0.000000 | 0.000000 |
| Fe | 0.000000 | -1.212783 | -0.000000 |
| Fe | 0.000000 | 1.212783 | 0.000000 |
| Fe | 2.068925 | -0.000000 | 0.000000 |
| Pb | -4.642258 | -1.617941 | 0.000000 |
| Pb | -4.642258 | 1.617941 | -0.000000 |
| Pb | -3.621362 | -0.000000 | 2.576613 |
| Pb | -3.621362 | 0.000000 | -2.576613 |
| Pb | -1.910992 | -2.570283 | -1.597852 |
| Pb | -1.910992 | -2.570283 | 1.597852 |
| Pb | -1.910992 | 2.570283 | -1.597852 |
| Pb | -1.910992 | 2.570283 | 1.597852 |
| Pb | 0.000000 | -0.000000 | 2.598173 |
| Pb | 0.000000 | 0.000000 | -2.598173 |
| Pb | 1.910992 | -2.570283 | -1.597852 |
| Pb | 1.910992 | -2.570283 | 1.597852 |
| Pb | 1.910992 | 2.570283 | -1.597852 |
| Pb | 1.910992 | 2.570283 | 1.597852 |
| Pb | 3.621362 | -0.000000 | 2.576613 |
| Pb | 3.621362 | 0.000000 | -2.576613 |
| Pb | 4.642258 | -1.617941 | 0.000000 |
| Pb | 4.642258 | 1.617941 | -0.000000 |

*D*$_{2h}$-[Fe$_4$Pb$_{18}$]$^{4-}$ ($^9$B$_{2u}$) **PBE**; S = 4; Bond Energy = -106.1882 eV
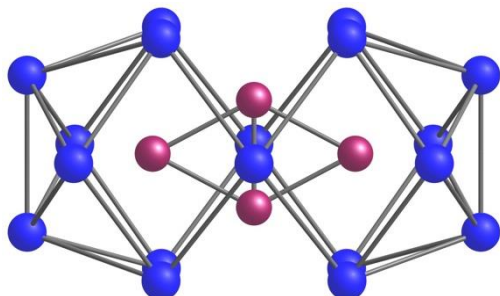


| Fe | -2.082254 | 0.000000 | 0.000000 |
| Fe | -0.000000 | -1.104596 | 0.000000 |
| Fe | 0.000000 | 1.104596 | 0.000000 |
| Fe | 2.082254 | -0.000000 | 0.000000 |

| Pb | -4.663880 | -1.612551 | 0.000000 |
|---|---|---|---|
| Pb | -4.663880 | 1.612551 | 0.000000 |
| Pb | -3.695469 | -0.000000 | -2.610716 |
| Pb | -3.695469 | -0.000000 | 2.610716 |
| Pb | -1.908389 | -2.483756 | -1.603867 |
| Pb | -1.908389 | -2.483756 | 1.603867 |
| Pb | -1.908389 | 2.483756 | -1.603867 |
| Pb | -1.908389 | 2.483756 | 1.603867 |
| Pb | 0.000000 | -0.000000 | 2.697926 |
| Pb | 0.000000 | 0.000000 | -2.697926 |
| Pb | 1.908389 | -2.483756 | -1.603867 |
| Pb | 1.908389 | -2.483756 | 1.603867 |
| Pb | 1.908389 | 2.483756 | -1.603867 |
| Pb | 1.908389 | 2.483756 | 1.603867 |
| Pb | 3.695469 | 0.000000 | -2.610716 |
| Pb | 3.695469 | 0.000000 | 2.610716 |
| Pb | 4.663880 | -1.612551 | 0.000000 |
| Pb | 4.663880 | 1.612551 | 0.000000 |

**$D_{2h}$-[Fe$_4$Sn$_{18}$]$^{4-}$ ($^{13}$B$_{3g}$) PBE**; S = 6; Bond Energy = -106.0472 eV
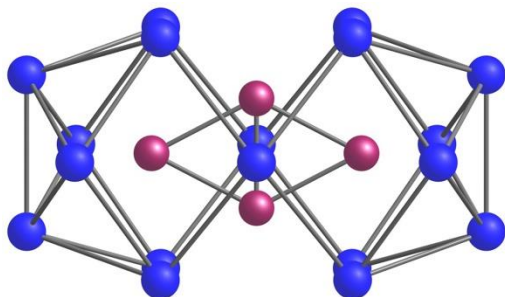


| Fe | -2.172123 | 0.000000 | 0.000000 |
|---|---|---|---|
| Fe | -0.000000 | 1.135559 | 0.000000 |
| Fe | 0.000000 | -1.135559 | 0.000000 |
| Fe | 2.172123 | -0.000000 | 0.000000 |
| Pb | -4.753193 | -1.624579 | 0.000000 |
| Pb | -4.753193 | 1.624579 | 0.000000 |
| Pb | -3.746434 | -0.000000 | -2.586399 |
| Pb | -3.746434 | -0.000000 | 2.586399 |
| Pb | -1.983773 | -2.505136 | -1.599545 |
| Pb | -1.983773 | -2.505136 | 1.599545 |
| Pb | -1.983773 | 2.505136 | -1.599545 |
| Pb | -1.983773 | 2.505136 | 1.599545 |
| Pb | 0.000000 | -0.000000 | 2.612914 |
| Pb | 0.000000 | 0.000000 | -2.612914 |
| Pb | 1.983773 | -2.505136 | -1.599545 |
| Pb | 1.983773 | -2.505136 | 1.599545 |

| Pb | 1.983773 | 2.505136 | -1.599545 |
|----|----------|----------|-----------|
| Pb | 1.983773 | 2.505136 | 1.599545 |
| Pb | 3.746434 | 0.000000 | -2.586399 |
| Pb | 3.746434 | 0.000000 | 2.586399 |
| Pb | 4.753193 | -1.624579 | 0.000000 |
| Pb | 4.753193 | 1.624579 | 0.000000 |

**$D_{2h}$-[Fe₄Sn₁₈]⁴⁻ ($^{11}B_{1g}$) PBE0**; S = 5; Bond Energy = -149.3374 eV
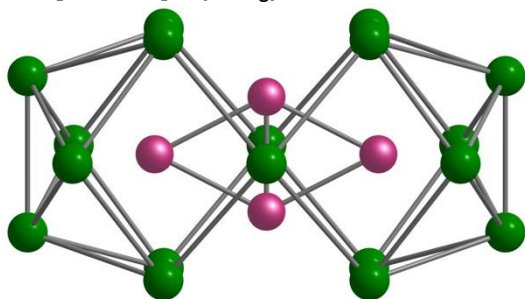


| Fe | -2.174304 | -0.000000 | 0.000000 |
|----|-----------|-----------|----------|
| Fe | -0.000000 | -1.117717 | 0.000000 |
| Fe | 0.000000 | 1.117717 | 0.000000 |
| Fe | 2.174304 | 0.000000 | 0.000000 |
| Sn | -4.643255 | -1.521250 | 0.000000 |
| Sn | -4.643255 | 1.521250 | 0.000000 |
| Sn | -3.758201 | -0.000000 | -2.510523 |
| Sn | -3.758201 | -0.000000 | 2.510523 |
| Sn | -2.000454 | -2.333553 | -1.569163 |
| Sn | -2.000454 | -2.333553 | 1.569163 |
| Sn | -2.000454 | 2.333553 | -1.569163 |
| Sn | -2.000454 | 2.333553 | 1.569163 |
| Sn | 0.000000 | -0.000000 | 2.535595 |
| Sn | 0.000000 | 0.000000 | -2.535595 |
| Sn | 2.000454 | -2.333553 | -1.569163 |
| Sn | 2.000454 | -2.333553 | 1.569163 |
| Sn | 2.000454 | 2.333553 | -1.569163 |
| Sn | 2.000454 | 2.333553 | 1.569163 |
| Sn | 3.758201 | 0.000000 | -2.510523 |
| Sn | 3.758201 | 0.000000 | 2.510523 |
| Sn | 4.643255 | -1.521250 | 0.000000 |
| Sn | 4.643255 | 1.521250 | 0.000000 |

**$D_{2h}$-[Fe₄Sn₁₈]⁴⁻ ($^{11}B_{3g}$) PBE0**; S = 5; Bond Energy = -149.6323 eV
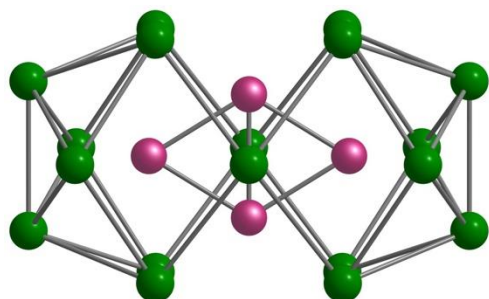
| Fe | -2.040166 | -0.000000 | 0.000000 |
|----|-----------|-----------|----------|
| Fe | -0.000000 | -1.259874 | 0.000000 |
| Fe | 0.000000 | 1.259874 | 0.000000 |
| Fe | 2.040166 | 0.000000 | 0.000000 |
| Sn | -4.492865 | -1.527314 | 0.000000 |
| Sn | -4.492865 | 1.527314 | 0.000000 |
| Sn | -3.533741 | 0.000000 | -2.483912 |
| Sn | -3.533741 | 0.000000 | 2.483912 |
| Sn | -1.907377 | -2.484114 | -1.548424 |
| Sn | -1.907377 | -2.484114 | 1.548424 |
| Sn | -1.907377 | 2.484114 | -1.548424 |
| Sn | -1.907377 | 2.484114 | 1.548424 |
| Sn | 0.000000 | -0.000000 | -2.462836 |
| Sn | 0.000000 | 0.000000 | 2.462836 |
| Sn | 1.907377 | -2.484114 | -1.548424 |
| Sn | 1.907377 | -2.484114 | 1.548424 |
| Sn | 1.907377 | 2.484114 | -1.548424 |
| Sn | 1.907377 | 2.484114 | 1.548424 |
| Sn | 3.533741 | -0.000000 | -2.483912 |
| Sn | 3.533741 | -0.000000 | 2.483912 |
| Sn | 4.492865 | -1.527314 | 0.000000 |
| Sn | 4.492865 | 1.527314 | 0.000000 |

The optimized cartesian coordinates of singlet $[Cu_4Sn_{18}]^{4-}$ and $[Cu_4Pb_{18}]^{4-}$, with corresponding bond energies. Stationary points were confirmed.

$D_{2h}$-$[Cu_4Sn_{18}]^{4-}$ ($^1A_g$); S = 0; Bond Energy = -99.1218 eV
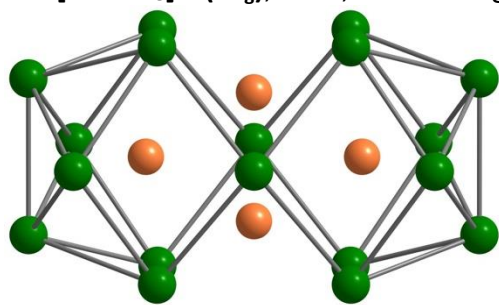


| Cu | -2.170049 | 0.000000 | 0.000000 |
|----|-----------|----------|----------|

| Cu | 0.000000 | -1.287470 | 0.000000 |
|----|----------|-----------|----------|
| Cu | 0.000000 | 1.287470 | 0.000000 |
| Cu | 2.170049 | 0.000000 | 0.000000 |
| Sn | -4.544207 | -1.593457 | 0.000000 |
| Sn | -4.544207 | 1.593457 | 0.000000 |
| Sn | -3.598326 | 0.000000 | -2.479774 |
| Sn | -3.598326 | 0.000000 | 2.479774 |
| Sn | -1.926917 | -2.439850 | -1.523581 |
| Sn | -1.926917 | -2.439850 | 1.523581 |
| Sn | -1.926917 | 2.439850 | -1.523581 |
| Sn | -1.926917 | 2.439850 | 1.523581 |
| Sn | 0.000000 | 0.000000 | -2.442321 |
| Sn | 0.000000 | 0.000000 | 2.442321 |
| Sn | 1.926917 | -2.439850 | -1.523581 |
| Sn | 1.926917 | -2.439850 | 1.523581 |
| Sn | 1.926917 | 2.439850 | -1.523581 |
| Sn | 1.926917 | 2.439850 | 1.523581 |
| Sn | 3.598326 | 0.000000 | -2.479774 |
| Sn | 3.598326 | 0.000000 | 2.479774 |
| Sn | 4.544207 | -1.593457 | 0.000000 |
| Sn | 4.544207 | 1.593457 | 0.000000 |

$D_{2h}$-[Cu$_4$Pb$_{18}$]$^{4-}$ ($^1A_g$); S = 0; Bond Energy = -94.1964 eV
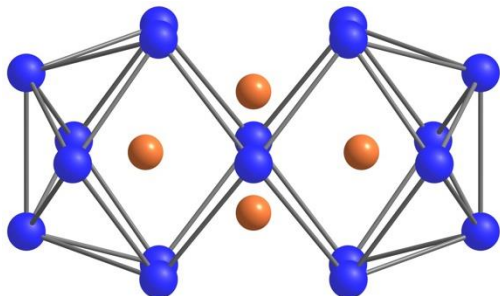


| Cu | -2.217917 | 0.000000 | 0.000000 |
|----|-----------|----------|----------|
| Cu | 0.000000 | -1.261034 | 0.000000 |
| Cu | 0.000000 | 1.261034 | 0.000000 |
| Cu | 2.217917 | 0.000000 | 0.000000 |
| Pb | -4.695226 | -1.660138 | 0.000000 |
| Pb | -4.695226 | 1.660138 | 0.000000 |
| Pb | -3.692693 | 0.000000 | -2.599921 |
| Pb | -3.692693 | 0.000000 | 2.599921 |
| Pb | -1.940274 | -2.537059 | -1.592346 |
| Pb | -1.940274 | -2.537059 | 1.592346 |
| Pb | -1.940274 | 2.537059 | -1.592346 |
| Pb | -1.940274 | 2.537059 | 1.592346 |
| Pb | 0.000000 | 0.000000 | -2.585181 |

| Pb | 0.000000 | 0.000000 | 2.585181 |
|----|----------|----------|----------|
| Pb | 1.940274 | -2.537059 | -1.592346 |
| Pb | 1.940274 | -2.537059 | 1.592346 |
| Pb | 1.940274 | 2.537059 | -1.592346 |
| Pb | 1.940274 | 2.537059 | 1.592346 |
| Pb | 3.692693 | 0.000000 | -2.599921 |
| Pb | 3.692693 | 0.000000 | 2.599921 |
| Pb | 4.695226 | -1.660138 | 0.000000 |
| Pb | 4.695226 | 1.660138 | 0.000000 |

The optimized cartesian coordinates of $[Pd_2Sn_{18}]^{4-}$, $[Fe_3Sn_{18}]^{4-}$, and $[Cd(NiSn_9)_2]^{6-}$, with corresponding bond energies. Stationary points were confirmed.

$D_{3d}$-$[Pd_2Sn_{18}]^{4-}$; S = 0; Bond Energy = -91.7270 eV
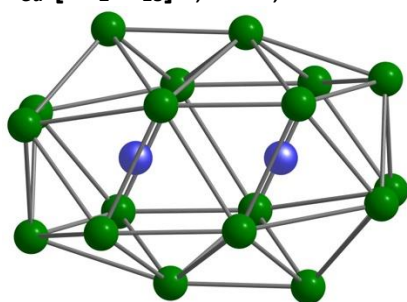


| Pd | -1.630976 | 0.000000 | -0.000000 |
|----|-----------|----------|-----------|
| Pd | 1.630976 | -0.000000 | 0.000000 |
| Sn | -3.990038 | -1.761383 | 0.000000 |
| Sn | -3.990038 | 0.880692 | -1.525403 |
| Sn | -3.990038 | 0.880692 | 1.525403 |
| Sn | -2.221834 | -1.442317 | -2.498166 |
| Sn | -2.221834 | -1.442317 | 2.498166 |
| Sn | -2.221834 | 2.884633 | 0.000000 |
| Sn | -0.866525 | -2.802840 | 0.000000 |
| Sn | -0.866525 | 1.401420 | -2.427331 |
| Sn | -0.866525 | 1.401420 | 2.427331 |
| Sn | 0.866525 | -1.401420 | -2.427331 |
| Sn | 0.866525 | -1.401420 | 2.427331 |
| Sn | 0.866525 | 2.802840 | -0.000000 |
| Sn | 2.221834 | -2.884633 | -0.000000 |
| Sn | 2.221834 | 1.442317 | -2.498166 |
| Sn | 2.221834 | 1.442317 | 2.498166 |
| Sn | 3.990038 | -0.880692 | -1.525403 |
| Sn | 3.990038 | -0.880692 | 1.525403 |
| Sn | 3.990038 | 1.761383 | -0.000000 |

$D_{3d}$-$[Fe_3Sn_{18}]^{4-}$; S = 3; Bonding Energy = -110.8432 eV
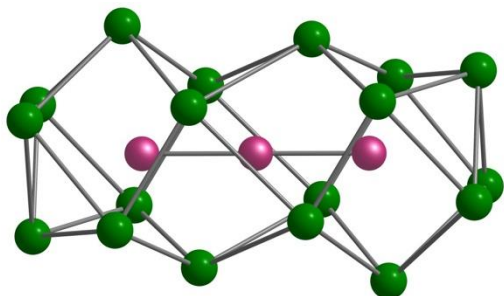
| Fe | -2.416679 | 0.000000 | -0.000000 |
|----|-----------|----------|-----------|
| Fe | 0.000000 | 0.000000 | 0.000000 |
| Fe | 2.416679 | -0.000000 | 0.000000 |
| Sn | -4.759765 | -1.758692 | -0.000000 |
| Sn | -4.759765 | 0.879346 | -1.523072 |
| Sn | -4.759765 | 0.879346 | 1.523072 |
| Sn | -2.801062 | -1.364018 | -2.362549 |
| Sn | -2.801062 | -1.364018 | 2.362549 |
| Sn | -2.801062 | 2.728036 | 0.000000 |
| Sn | -1.223809 | -2.438309 | -0.000000 |
| Sn | -1.223809 | 1.219155 | -2.111638 |
| Sn | -1.223809 | 1.219155 | 2.111638 |
| Sn | 1.223809 | -1.219155 | -2.111638 |
| Sn | 1.223809 | -1.219155 | 2.111638 |
| Sn | 1.223809 | 2.438309 | 0.000000 |
| Sn | 2.801062 | -2.728036 | -0.000000 |
| Sn | 2.801062 | 1.364018 | -2.362549 |
| Sn | 2.801062 | 1.364018 | 2.362549 |
| Sn | 4.759765 | -0.879346 | -1.523072 |
| Sn | 4.759765 | -0.879346 | 1.523072 |
| Sn | 4.759765 | 1.758692 | 0.000000 |

$D_{3d}$-[Cd(NiSn$_9$)$_2$]$^{6-}$; S = 0; Bonding Energy = -101.3659 eV
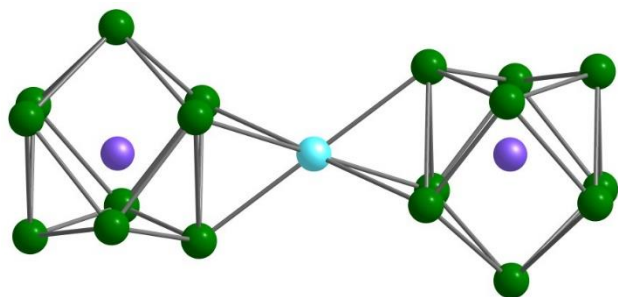


| Cd | 0.000000 | 0.000000 | 0.000000 |
|----|----------|----------|----------|
| Ni | -4.268052 | -0.000000 | 0.000000 |
| Ni | 4.268052 | 0.000000 | -0.000000 |
| Sn | -6.171905 | -0.903532 | -1.564964 |
| Sn | -6.171905 | -0.903532 | 1.564964 |

```
Sn    -6.171905     1.807064     0.000000
Sn    -4.290071    -2.743711     0.000000
Sn    -4.290071     1.371856    -2.376124
Sn    -4.290071     1.371856     2.376124
Sn    -2.501178    -0.948112     1.642179
Sn    -2.501178    -0.948112    -1.642179
Sn    -2.501178     1.896225    -0.000000
Sn     2.501178    -1.896225     0.000000
Sn     2.501178     0.948112    -1.642179
Sn     2.501178     0.948112     1.642179
Sn     4.290071    -1.371856    -2.376124
Sn     4.290071    -1.371856     2.376124
Sn     4.290071     2.743711    -0.000000
Sn     6.171905    -1.807064    -0.000000
Sn     6.171905     0.903532    -1.564964
Sn     6.171905     0.903532     1.564964
```

## 7. References

[1]   G. Sheldrick, *Acta. Cryst. A.*, 2015, **71**, 3-8.

[2]   O. V. Dolomanov, L. J. Bourhis, R. J. Gildea, J. A. K. Howard, H. Puschmann, *J. Appl. Crystallogr.* **42**, 339-341 (2009).

[3]   A. Spek, *Acta. Cryst. D.*, 2009, **65**, 148-155.

[4]   A. Spek, *Acta. Cryst. C.*, 2015, **71**, 9-18.

[5]   J. P. Perdew, K. Burke, M. Ernzerhof, *Phys. Rev. Lett.*, 1996, **77**, 3865-3868.

[6]   M. Ernzerhof, G. E. Scuseria, *J. Chem. Phys.*, 1999, **110**, 5029-5036.

[7]   S. Grimme, *J. Comput. Chem.*, 2004, **25**, 1463-1473.

[8]   Z.-S. Li, W.-X. Chen, H. W. T. Morgan, C.-C. Shu, J. E. McGrady and Z.-M. Sun, *Chem. Sci.*, 2024, **15**, 1018-1026.

[9]   Y.-N. Yang, L. Qiao and Z.-M. Sun, *Chin. Chem. Lett.*, 2023, **34**, 107207.

[10] Z.-M. Sun, H. Xiao, J. Li and L.-S. Wang, *J. Am. Chem. Soc.,* 2007, **129**, 9560-9561.

[11] F. K. Sheong, W.-J. Chen, J.-X. Zhang, Y. Li and Z. Lin, *Dalton Trans.*, 2017, **46**, 2214–2219.

[12] J.-X. Zhang, F. K. Sheong and Z. Lin, *Inorg. Chem.*, 2019, **58**, 3473–3478.

[13] J.-X. Zhang, F. K. Sheong and Z. Lin, *WIREs Comp. Mol. Sci.*, 2020, **10**, e1469.

[14] L. Qiao, C. Zhang, C.-C. Shu, H. W. T. Morgan, J. E. McGrady and Z.-M. Sun, *J. Am. Chem. Soc.*, 2020, **142**, 13288–13293.